axioms

MDPI

Article

Chaotic Motions in Linear/Nonlinear and Quasi-Periodical Dynamic Systems Revealed by Energy-Flow Investigations

Jing Tang Xing [1,*] and Wei Dai [2]

[1] Civil Maritime Environmental Engineering, Faculty of Engineering & Physical Sciences, University of Southampton, Southampton SO17 1BJ, UK
[2] School of Naval Architecture and Ocean Engineering, Huazhong University of Science and Technology, 1037 Luoyu Road, Wuhan 430074, China; daiwei699@hust.edu.cn
* Correspondence: jtxing@soton.ac.uk

Abstract

By using 1~2 degrees of freedom (DOF) examples, linear/nonlinear and quasi-periodical systems (QPS) are investigated based on the energy-flow theory (EFT), which reveals the following new findings on chaotic motions. (a) A 1-DOF linear non-damped-forced motion is chaotic if there is no least common multiple (LCM) for the periods of natural and force frequencies. (b) For a 1-DOF nonlinear non-damping-forced system with nonlinear stiffness of $\gamma x^2, (\gamma > 0)$, both the free vibration by initial conditions and the composed motion with forced one excited by a force of given frequency are chaotic; while, when damping is added, the free vibration is damped to zero, but the forced vibration consists of different frequency components showing chaotic characteristics. (c) For a 1-DOF system of natural frequency 1 with nonlinear damping $2\varepsilon(\dot{x}) = -2 + \dot{x} + \dot{x}^2, \varepsilon(\dot{x}) < 0, \varepsilon(\dot{x})^2 < 1$, the free vibration by the initial conditions $(x_0 = 1, p_0 = 0)$ is along a non-repeating orbit towards a zero energy-flow limit circle of $\dot{E} = 0,\ p = -1$. The tackled 1-DOF systems of no LCMs belong to a type of QPS, which implies that the orbit of a QPS in the phase space is also a non-closed curve, and based on the EFT, its motion is chaotic. The chaotic orbits of above 1-DOF cases in the phase space, as well as a 2-DOF free vibration case, are numerically examined to confirm the theoretical prediction. The findings may suggest that the LCMs could be an important factor in identifying chaotic motions. It is demonstrated that the generalised potential energy (GPE) and the energy-flow characteristic factors (EFCF), respectively, play a Lyapunov function and exponents to tackle the stabilities and chaotic motions of dynamic systems.

Keywords: linear chaotic motion; chaos identifications; nonlinear stiffness/damping; least common multiple (LCM); chaotic orbit of QPS; Lyapunov function and exponents

MSC: 74H65; 37C56

Check for updates

Academic Editors: Elena-Corina Cipu and Cosmin Dănuț Barbu

Received: 31 May 2026
Revised: 10 July 2026
Accepted: 11 July 2026
Published: 14 July 2026

Copyright: © 2026 by the authors. Licensee MDPI, Basel, Switzerland. This article is an open access article distributed under the terms and conditions of the Creative Commons Attribution (CC BY) license.

1. Introduction

In mathematics and physics, chaos is considered an inherent characteristic of nonlinear dynamical systems (NDS). An early proponent of chaos theory was Poincare [1]. In the 1880s, while studying the three-body problem, he found that there can be orbits which are non-periodic, and yet not forever increasing or approaching a fixed point [2]. However, this proponent did not cause more attention from scientists and engineers until Lorenz [3], an early pioneer of the theory, whose interest in chaos came about accidentally through his work on weather prediction. After Lorenz's discovery, investigations into chaos have

developed very fast. There have been many books and papers highlighting its origin, developments and possible future directions, for example, the publications [4–16]. In these books, the two most influential books could be by Stroyatz [17] and Larek [18]. The former presents a very good introductory text in nonlinear dynamics and chaos, emphasising applications in several areas of science, including vibrations, biological rhythms, insect outbreaks, and genetic control systems, and contains a rich selection of illustrations, with many exercises and examples. The latter discusses continuous and discrete nonlinear systems in systematic and sequential approaches, with its unique feature being mathematical theories on analysis of nonlinear systems and chaos routes, and the new edition includes some new topics, such as centre manifold reduction, new active research direction on organised structures for transitional and chaotic regimes and the connections of complex chaotic attractors with fractal cascades. Both books could be chosen as textbooks for different levels of students in engineering and mathematics. The interested readers may wish to consult these two books for more detailed discussions on chaos theories and applications, as well as more useful references. For obtaining more newly discovered hidden nonlinear chaotic phenomena, the conferences would be the most important places to fast collect them, of which some series conferences with the electronic proceedings organised and published by Springer Nature are more influential in the world, for example, the series conference monographs [19–22].

"Chaos" is normally understood as "a state of disorder". However, in chaos theory, the term is defined more precisely. Although there is no universally accepted mathematical definition of chaos, a commonly used definition says that, for a dynamical system to be classified as chaotic, it must have some properties indicated by Hasselblatt & Katok [23], such as being sensitive to initial conditions, topological transitivity and dense 'periodic' orbits.

According to the author's knowledge, in all publications before 2015, the chaotic motions are identified by the Lyapunov exponents or Poincare maps, of which the detailed methods and mathematical formulations can be read in the books [17,18]. For example, in many recent publications [24–29] involving vibration reductions by nonlinear isolators or nonlinear energy sinks, these two historic approaches are still used to reveal the chaotic/bifurcation characteristics of NDS. In 2015, Xing [30] developed a generalised means, the energy-flow theory (EFT), to investigate any types of NDS in macroscopic, microscopic and mesoscopic fields in nature and engineering [30–37]. Based on this theory, chaotic motions can be identified by some energy-flow criteria [30,32] summarised later, which have been demonstrated to be very effective by examining the well-known chaotic motions [30,32], such as Van Der Pol Oscillator [38,39], Duffing's system [40], SD oscillator [41,42], Lorenz system [43,44] and Rössler oscillator [45]. In the recent papers [46,47] studying the three-body problems and the motions in the gravity fields, this method has revealed the chaotic motions in Newton's gravity field.

In recent years, with the fast development of computer/network techniques and application requirements, an attractive and imperative topic called chaos synchronisation has been investigated and developed [48–52], for which a review of different synchronisation methods has been reported [53]. The chaotic synchronisation signifies a process to track the trajectory of the master chaotic response, so that it closely involves chaos identification. Aiming to reveal a lock-in regime where the vortex frequency coincides with the structure one, paper [54] reported a large eddy numerical simulation of a wind–structure interaction system to avoid self-excited large vibrations, which concerns tackling the stability of the system. As good effective research, paper [55] proposed a generalised van der Pol model with metastability/chaos identifications by examining their defined potential energy E and its time derivative $\dot{E}$, which is just the generalised potential energy (GPE) and its energy flows developed and used to tackle NDS by the author [30–37]. Although their paper has

not used the full EFT given in [30–37], it has partially demonstrated the efficiency of the EFT to reveal the inherent behaviour of NDS. To list too many publications in different areas concerning stabilities/chaos/vortex identifications of dynamic systems, the interested readers may refer to the above-given references with their cited original information to obtain more details of the topics discussed in this paper.

Reading the publications on chaos, we have the following questions to be addressed. The first one concerns whether chaotic motions can appear in linear systems. This is proposed based on the facts: in current publications, there are no reports on chaos revealed in linear systems. The second question is to ask us what the conditions are to generate chaotic motions in dynamic systems. The current reports only show finding various chaotic motions, but we do not know any mechanisms that cause chaotic motions. In a preprint paper [56], these problems were initially tackled by investigating 1-DOF linear/nonlinear and quasi-periodical dynamic systems based on the EFT with theoretical analysis and numerical simulations. This paper is the new modified version of preprint [56], in which, following the introduction, Section 2 gives the fundamentals of EFT used in the next sections, in which GPE and EFCF are demonstrated to play the roles of Lyapunov function and exponents by using the principal energy-flow space (PEFS). Section 3 investigates a 1-DOF system in three cases: one is a linear system, two are nonlinear systems with nonlinear stiffness and damping. A generalised 1-DOF linear and nonlinear non-dimensional dynamic system can be represented as

$$\ddot{x} + 2\varepsilon(x,\dot{x})\dot{x} + \omega^2(x,\dot{x})x = F(\tau) = \widetilde{F}\cos\widetilde{\omega}\tau, \quad \omega \neq 0, \tag{1}$$

where $\varepsilon(x,\dot{x})$, $\omega^2(x,\dot{x})$ and $F(\tau)$ respectively denote the non-dimensional damping, stiffness and excitation force of frequency $\widetilde{\omega}$ and amplitude $\widetilde{F}$ of the system. For linear systems, the damping and stiffness are constants, while for nonlinear systems, they are functions of dynamic variables. Section 4 investigates quasi-periodical systems (QPS). Section 5 gives a detailed discussion, based on the commonly accepted knowledge, the Poincare maps, the Lyapunov exponents and the mentioned orbit characteristics, to further confirm that the revealed chaotic motions in a 1-DOF linear system are acceptable.

2. Fundamentals of Energy-Flow Theory [30–37]

2.1. State Equation in the Phase Space

Equation (1) can be represented in the form of a phase space:

$$\begin{bmatrix} \dot{x} \\ \dot{p} \end{bmatrix} = \begin{bmatrix} 0 & 1 \\ -\omega^2 & -2\varepsilon \end{bmatrix} \begin{bmatrix} x \\ p \end{bmatrix} + \begin{bmatrix} 0 \\ F \end{bmatrix}. \tag{2}$$

2.2. Energy-Flow Variables

The generalised potential energy (GPE) (E) and the generalised kinetic energy (GKE) (K) are, respectively, defined as

$$E = \frac{1}{2}(x^2 + p^2), \qquad K = \frac{1}{2}(\dot{x}^2 + \dot{p}^2), \tag{3}$$

which are two positive real variables. Physically, GPE concerns the potential/kinetic energies, and geometrically, it involves the position and distance d of a phase point (x, p) to the origin of phase space, i.e.,

$$d = \sqrt{2E}, \tag{4}$$

so that we call it as generalised potential energy, the variable K geometrically involves the tangent vector at a point on the orbit in the phase space. As shown in Figure 1, where $\boldsymbol{g}_1$ and $\boldsymbol{g}_2$ respectively denote the unit vectors along the two-coordinate x and p directions, so that at a point A (x, p) on the orbit, the position vector and the tangent vector are

$$\boldsymbol{r} = x\boldsymbol{g}_1 + p\boldsymbol{g}_2, \quad E = \frac{1}{2}\boldsymbol{r}\cdot\boldsymbol{r}, \ \boldsymbol{\tau} = \dot{\boldsymbol{r}} = \dot{x}\boldsymbol{g}_1 + \dot{p}\boldsymbol{g}_2, \quad K = \frac{1}{2}\dot{\boldsymbol{r}}\cdot\dot{\boldsymbol{r}}. \tag{5}$$

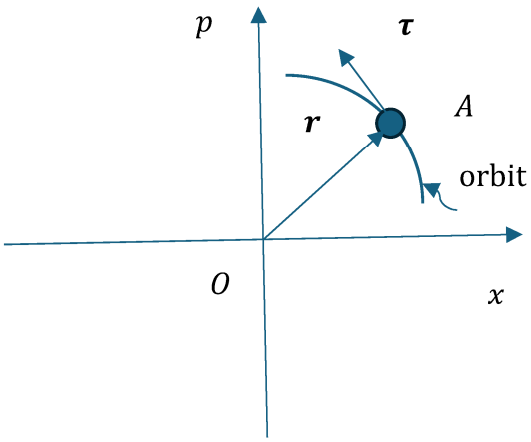


Figure 1. The position and tangent vectors of the point A on the orbit in the phase space.

Therefore, we have

$$d = |\boldsymbol{r}| = \sqrt{2E}, \qquad |\boldsymbol{\tau}| = \sqrt{\dot{x}^2 + \dot{p}^2} = \sqrt{2K}. \tag{6}$$

2.3. Energy Flow Equation (EFE) and Energy Flow Matrix (EFM)

Multiplying Equation (2) by the row vector $\begin{bmatrix} x & p \end{bmatrix}$, we obtain a potential EFE

$$\dot{E} = \begin{bmatrix} x & p \end{bmatrix}\begin{bmatrix} \dot{x} \\ \dot{p} \end{bmatrix} = \begin{bmatrix} x & p \end{bmatrix}\begin{bmatrix} 0 & 1 \\ -\omega^2 & -2\varepsilon \end{bmatrix}\begin{bmatrix} x \\ p \end{bmatrix} + \begin{bmatrix} x & p \end{bmatrix}\begin{bmatrix} 0 \\ F \end{bmatrix}, \tag{7}$$

$$\dot{E} = \boldsymbol{r}\cdot\dot{\boldsymbol{r}}, \qquad \ddot{E} = 2K + \boldsymbol{r}\cdot\ddot{\boldsymbol{r}},$$

which can be further written as

$$\dot{E} = \begin{bmatrix} x & p \end{bmatrix}(\boldsymbol{E}+\boldsymbol{U})\begin{bmatrix} x \\ p \end{bmatrix} + \begin{bmatrix} x & p \end{bmatrix}\begin{bmatrix} 0 \\ F \end{bmatrix} = \begin{bmatrix} x & p \end{bmatrix}(\boldsymbol{E})\begin{bmatrix} x \\ p \end{bmatrix} + \begin{bmatrix} x & p \end{bmatrix}\begin{bmatrix} 0 \\ F \end{bmatrix}, \qquad \begin{bmatrix} x & p \end{bmatrix}(\boldsymbol{U})\begin{bmatrix} x \\ p \end{bmatrix} \equiv 0, \tag{8}$$

$$\boldsymbol{E} = \frac{1}{2}\begin{bmatrix} 0 & 1-\omega^2 \\ 1-\omega^2 & -4\varepsilon \end{bmatrix}, \qquad \boldsymbol{U} = \frac{1}{2}\begin{bmatrix} 0 & 1+\omega^2 \\ -1-\omega^2 & 0 \end{bmatrix}.$$

Time change rate of phase volume strain $\quad \dot{v} = \mathrm{Trice}(\boldsymbol{E}) = -2\varepsilon.$

Here, the matrix $\boldsymbol{E}$ is a real symmetric matrix called the EFM of the system, while the matrix $\boldsymbol{U}$ is a real anti-symmetric matrix defined as a spin matrix (SM).

Similarly, taking a time derivative of GKE K in Equation (3) in association with Equation (2), we obtain a kinetic EFE:

$$\dot{K} = \begin{bmatrix} \dot{x} & \dot{p} \end{bmatrix}\begin{bmatrix} \ddot{x} \\ \ddot{p} \end{bmatrix} = \begin{bmatrix} \dot{x} & \dot{p} \end{bmatrix}\begin{bmatrix} 0 & 1 \\ -\omega^2 & -2\varepsilon \end{bmatrix}\begin{bmatrix} \dot{x} \\ \dot{p} \end{bmatrix} + \begin{bmatrix} \dot{x} & \dot{p} \end{bmatrix}\begin{bmatrix} 0 & 0 \\ -2\omega\dot{\omega} & -2\dot{\varepsilon} \end{bmatrix}\begin{bmatrix} x \\ p \end{bmatrix} + \begin{bmatrix} \dot{x} & \dot{p} \end{bmatrix}\begin{bmatrix} 0 \\ \dot{F} \end{bmatrix} \tag{9}$$

$$= \begin{bmatrix} \dot{x} & \dot{p} \end{bmatrix} \boldsymbol{E} \begin{bmatrix} \dot{x} \\ \dot{p} \end{bmatrix} + \dot{p}\left(\dot{F} - 2\dot{\varepsilon}p - 2\omega\dot{\omega}x\right), \qquad \dot{K} = \dot{\boldsymbol{r}}\cdot\ddot{\boldsymbol{r}}.$$

2.4. Energy-Flow Characteristic Factor (EFCF) and Principal Energy-Flow Space (PEFS)

2.4.1. EFCF and Energy-Flow Characteristic Vector (EFCV)

The real symmetric EFM $\boldsymbol{E}$ has real eigenvalues λ and the corresponding eigenvectors $\boldsymbol{\phi}$ derived by the equation

$$\boldsymbol{E\phi} = \lambda\boldsymbol{\phi}, \qquad |\boldsymbol{E} - \boldsymbol{\lambda I}| = 0. \tag{10}$$

Here λ and $\boldsymbol{\phi}$ are, respectively, defined as EFCF and EFCV, which satisfy the orthogonality relationship

$$\boldsymbol{\phi}_J^T \boldsymbol{E\phi_I} = \lambda_I \delta_{IJ}, \qquad \boldsymbol{\phi}_J^T \boldsymbol{\phi_I} = \delta_{IJ} = \begin{cases} 1, & I = J \\ 0, & I \neq J \end{cases}, \tag{11}$$

where δ_{IJ} is Kronecker Delta [57]. Substituting EFM in Equation (8) into Equation (10), we obtain

$$\begin{vmatrix} -\lambda & 0.5(1-\omega^2) \\ 0.5(1-\omega^2) & -2\varepsilon - \lambda \end{vmatrix} = \lambda^2 + 2\varepsilon\lambda - \frac{1}{4}\left(1-\omega^2\right)^2 = 0, \tag{12}$$

which gives

$$\lambda_{1,2} = \frac{-2\varepsilon \mp \sqrt{4\varepsilon^2 + (1-\omega^2)^2}}{2} = \varepsilon\left\{-1 \mp \sqrt{1 + \left(\frac{1-\omega^2}{2\varepsilon}\right)^2}\right\}, \qquad \lambda_1 < 0, \quad \lambda_2 > 0, \quad \dot{v} = \lambda_1 + \lambda_2 = -2\varepsilon, \tag{13}$$

$$\boldsymbol{\phi}_I = \frac{1}{\sqrt{1+\varphi_I^2}} \begin{bmatrix} 1 \\ \varphi_I \end{bmatrix}, \qquad \varphi_I = \frac{2\lambda_I}{1-\omega^2}, \qquad I = 1, 2.$$

2.4.2. PEFS

The orthogonal EFCV spans a PEFS to describe the motion of the system. Generally, PEFS is dependent on the positions in the phase space, because EFCVs are functions of positions. We discuss the motions of the system in PEFS in the two aspects.

- Linear case: EFCFs and EFCVs are constants, so that EFCVs, as the fixed coordinate axis, define the principal energy-flow direction (PEFD) to describe the motion of a phase space point. The position and velocity of a point can be expressed as

$$\begin{bmatrix} x \\ p \end{bmatrix} = \boldsymbol{\Phi\eta}, \qquad \boldsymbol{\eta} = \begin{bmatrix} \eta_1 \\ \eta_2 \end{bmatrix}, \qquad \begin{bmatrix} \dot{x} \\ \dot{p} \end{bmatrix} = \boldsymbol{\Phi}\dot{\boldsymbol{\eta}}, \qquad \boldsymbol{\Phi} = \begin{bmatrix} \boldsymbol{\phi_1} & \boldsymbol{\phi_2} \end{bmatrix}, \tag{14}$$

  where η_I denotes the coordinates of a phase point. Substituting Equation (14) into EFE Equation (8) and then using Equation (11), we obtain EFE in PEFS as

$$\dot{\boldsymbol{\eta}} = \boldsymbol{\Phi}^T \boldsymbol{E\Phi} \begin{bmatrix} \eta_1 \\ \eta_2 \end{bmatrix} + \boldsymbol{\Phi}^T \begin{bmatrix} 0 \\ F \end{bmatrix} = \boldsymbol{diag}(\lambda)\boldsymbol{\eta} + \boldsymbol{F}, \qquad \boldsymbol{F} = \begin{bmatrix} F_1 \\ F_2 \end{bmatrix} = \boldsymbol{\Phi}^T \begin{bmatrix} 0 \\ F \end{bmatrix}, \tag{15}$$

  so that we have the following two independent motion equations

$$\dot{\eta}_I = \lambda_I \eta_I + F_I, \tag{16}$$

as well as GPE/GKE with their EFEs in the forms

$$E = \frac{1}{2}\boldsymbol{\eta}^T\boldsymbol{\eta}, \qquad \dot{E} = \boldsymbol{\eta}^T\dot{\boldsymbol{\eta}} = \boldsymbol{\eta}^T\boldsymbol{diag}(\lambda)\boldsymbol{\eta} + \boldsymbol{\eta}^T\boldsymbol{F}, \tag{17}$$

$$K = \frac{1}{2}\dot{\boldsymbol{\eta}}^T\dot{\boldsymbol{\eta}}, \qquad \dot{K} = \dot{\boldsymbol{\eta}}^T\ddot{\boldsymbol{\eta}} = \dot{\boldsymbol{\eta}}^T\boldsymbol{diag}(\lambda)\dot{\boldsymbol{\eta}} + \dot{\boldsymbol{\eta}}^T\dot{\boldsymbol{F}}.$$

From Equations (16) and (17), when we consider the inherent behaviour without any external forces, it follows

$$d\eta_I = \lambda_I\eta_I d\tau, \quad \frac{d\eta_I}{\eta_I} = \lambda_I d\tau, \quad \eta_I = \eta_{I0}e^{\lambda_I\tau}, \quad \eta_{I0} = \eta_I(\tau = 0), \tag{18}$$

$$\dot{E} = \lambda_1\eta_1^2 + \lambda_2\eta_2^2, \quad \dot{K} = \lambda_1\dot{\eta}_1^2 + \lambda_2\dot{\eta}_2^2,$$

which independently govern the motions of the phase point along each PEFD.

- Nonlinear case: EFM, EFCF, and the principal eigenvectors of EFM are the functions of time, so that for different points at time $\hat{\tau}$ in the phase space, EFCF $\hat{\lambda}_I$ and EFCV $\hat{\boldsymbol{\phi}}_{\boldsymbol{I}}$ are different. To use EFT to investigate the dynamic behaviour in a small domain around a point, the linearised form of the nonlinear equation at this point can be used (see details in [30]). For the linearised equation, the Jacobin and EFM in the small domain of the point are considered as constants, so that EFCVs $\hat{\boldsymbol{\phi}}_{\boldsymbol{I}}$ are constants, and span a local PEFS in the small domain around the point, in which the motions of the phase point in this small domain can be tackled. Therefore, if we replace the related variables, matrices in Equations (14)–(18), with the corresponding ones marked by "ˆ", we can obtain all equations governing the behaviour of the system in the local small domain. For example, Equation (18) now becomes

$$d\hat{\eta}_I = \hat{\lambda}_I\hat{\eta}_I d\tau, \quad \frac{d\hat{\eta}_I}{\hat{\eta}_I} = \hat{\lambda}_I d\tau, \quad \hat{\eta}_I = \hat{\eta}_{I0}e^{\hat{\lambda}_I\tau}, \quad \hat{\eta}_{I0} = \hat{\eta}_I(\tau = \hat{\tau}), \tag{19}$$

in which the time integration starts from time $\hat{\tau}$, not the initial time $\tau = 0$.
In the following discussions, for our convenience, we will omit the hat "ˆ" to mark the nonlinear case concerning local small areas, but just use the notations in Equations (14)–(18). Therefore, when the nonlinear case is concerned, we should remember that the related variables with the omitted hat "ˆ" are restricted in a small domain around a point.

2.4.3. Moving Direction of Phase Point and Energy-Flow Surface

Based on Equations (14)–(19), and the geometrical meaning of GPE in Equation (4), as well as noting the two EFCFs ($\lambda_1 < 0,\ \lambda_2 > 0$) in Equation (13), we can conclude that for the case of no excitation force F,

$$\dot{E} =: \begin{cases} < 0, & \eta_1^2 = \eta_2^2 \text{ or } \eta_2^2 = 0,\ \eta_1^2 \neq 0, \\ > 0, & \eta_1^2 = 0,\ \eta_2^2 \neq 0, \\ = 0, & \lambda_1\eta_1^2 + \lambda_2\eta_2^2 = 0, \end{cases} \tag{20}$$

which implies the distance of a phase space point, to the origin or the local reference point, decreases, increases and remains the same, respectively.

The EFS are hyperbolic surfaces formulated by

$$\lambda_2\eta_2^2 - |\lambda_1|\eta_1^2 = \dot{E}, \qquad \frac{\eta_2^2}{1/\lambda_2} - \frac{\eta_1^2}{1/|\lambda_1|} = \dot{E}, \tag{21}$$

as shown in Figure 2(I), and the zero energy-flow lines (ZEFL) are determined by

$$\dot{E} = \lambda_1 \eta_1^2 + \lambda_2 \eta_2^2 = 0, \tag{22}$$

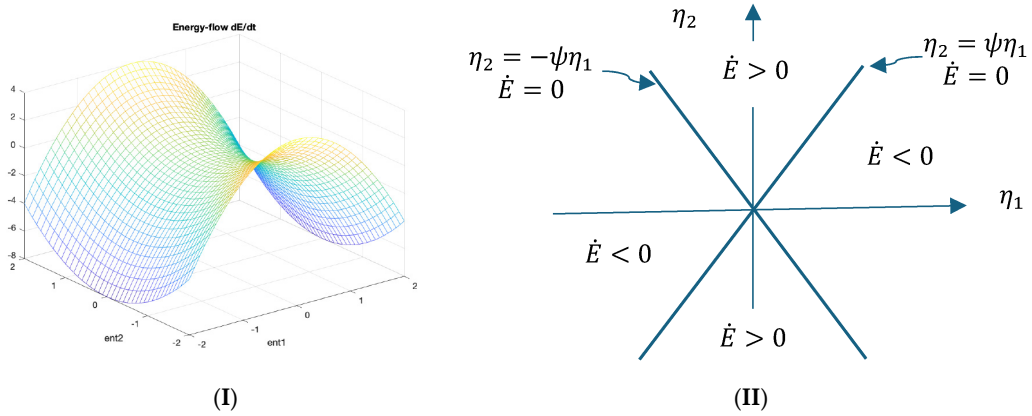
that is

$$\left(\sqrt{-\lambda_1}\right)^2 \eta_1^2 - \left(\sqrt{\lambda_2}\right)^2 \eta_2^2 = \left(\sqrt{-\lambda_1}\eta_1 - \sqrt{\lambda_2}\eta_2\right)\left(\sqrt{-\lambda_1}\eta_1 + \sqrt{\lambda_2}\eta_2\right) = 0, \tag{23}$$

implying the two ZEFLs governed by

$$\eta_2 = \pm\psi\eta_1, \qquad \psi = \frac{\sqrt{-\lambda_1}}{\sqrt{\lambda_2}}, \tag{24}$$

shown in Figure 2(II), which divides EFS into 4 domains with positive or negative energy flows.



(I) **(II)**

Figure 2. **(I)** The hyperbolic surface ($\lambda_1 = -2,\ \lambda_2 = 1$); **(II)** the two ZEFLs in Equation (24) divide the space into 4 domains with positive or negative energy-flows.

2.5. Energy Flow Characteristics

2.5.1. Equilibrium Point (EP)

From Equation (2) of $F = 0$, the EP of the system is defined by

$$\begin{bmatrix} \dot{x} \\ \dot{p} \end{bmatrix} = \begin{bmatrix} 0 & 1 \\ -\omega^2 & -2\varepsilon \end{bmatrix} \begin{bmatrix} x \\ p \end{bmatrix} = 0, \qquad p = 0, \quad x = 0, \tag{25}$$

which gives a point $p = 0 = x$ in the phase space, the origin of phase space is an EP.

2.5.2. ZEFS and Stability

Vanishing the flow of GPE in Equation (8), we have ZEFS defined by

$$\dot{E} = \begin{bmatrix} x & p \end{bmatrix} \begin{bmatrix} 0 & 0.5(1-\omega^2) \\ 0.5(1-\omega^2) & -2\varepsilon \end{bmatrix} \begin{bmatrix} x \\ p \end{bmatrix} + \begin{bmatrix} x & p \end{bmatrix} \begin{bmatrix} 0 \\ F \end{bmatrix} = 0, \qquad E = \hat{E} = \text{constant}, \tag{26}$$

$$\left[\left(1-\omega^2\right)x - 2\varepsilon p + F\right] p = 0,$$

implying the velocity vector is perpendicular to the force, so that the energy flow is zero, and the distance of the phase point to the origin is a constant.

Geometrically, GPE E relating the distance of the phase point to the origin or to a local point, so that it provides a *Lyapunov function* to tackle the local stability of equilibrium points and the point on ZEFS, as shown in Figure 3. To judge the local stability of a point

on EP or on ZEFS, we can investigate the energy flows at a shifting position from the point in the small domain. From Equation (18), in PEFS, we have

$$\dot{E} = \lambda_1\eta_1^2 + \lambda_2\eta_2^2, \quad E = \frac{1}{2}\left(\eta_1^2 + \eta_2^2\right), \quad \dot{K} = \lambda_1\dot{\eta}_1^2 + \lambda_2\dot{\eta}_2^2, \quad K = \frac{1}{2}\left(\dot{\eta}_1^2 + \dot{\eta}_2^2\right), \quad \eta_I = \eta_{I0}e^{\lambda_I\tau}, \tag{27}$$

where the last one gives the time function of η_I in the *I-th* PEFD, which theoretically confirms that EFCF λ_I exactly plays the role of Lyapunov exponents. Therefore, for any NDSs, GPE automatically plays the role of Lyapunov function, and EFCF as Lyapunov exponents to reveal its inherent dynamic behaviours, including stability, possible periodical orbit and chaotic motions being addressed below.

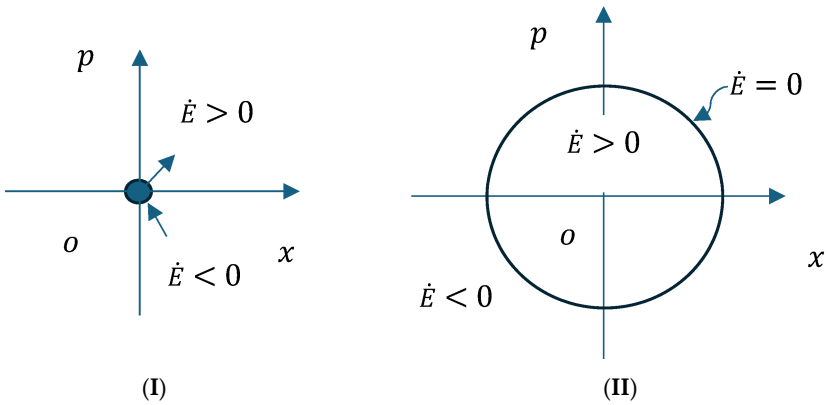


Figure 3. (**I**) The stability of EP *o*: a point shifted from *o*, if $\dot{E} > 0$, moves far from the origin so that EP is not stable, while if $\dot{E} < 0$, it moves back to the origin, and it is stable. (**II**) The stability of a ZEFS: a disturbance causes a point to shift from ZEFS, if $\dot{E} > 0$ inside the surface, and $\dot{E} < 0$ outside of the surface, this surface is stable; it is not stable.

2.5.3. Periodical Orbits (POs)

For a PO, a phase point at time $\hat{\tau}$ must go back to the same point after a period T, i.e.,

$$\begin{bmatrix} x \\ p \end{bmatrix}(\hat{\tau}) = \begin{bmatrix} x \\ p \end{bmatrix}(\hat{\tau} + \mathrm{T}), \qquad E(\hat{\tau}) = E(\hat{\tau} + \mathrm{T}), \qquad \dot{E}(\hat{\tau}) = \dot{E}(\hat{\tau} + \mathrm{T}), \tag{28}$$

$$K(\hat{\tau}) = K(\hat{\tau} + \mathrm{T}), \qquad \dot{K}(\hat{\tau}) = \dot{K}(\hat{\tau} + \mathrm{T}).$$

Based on EFT, a necessary condition of POs is that SM does not vanish, i.e.,

$$\mathbf{U} \neq \mathbf{0}, \tag{29}$$

which is shown in Equation (8). Also, the two Lyapunov exponents λ_I, one positive and another negative, so that there exist POs possibly. To confirm it, we must check if the following time-averaged generalised potential energy (TAGPE), the time-averaged generalised kinetic energy (TAGKE), and their time-averaged energy-flows (TAEFs) satisfy the criteria,

$$\langle E \rangle = \frac{1}{T}\int_{\hat{\tau}}^{T+\hat{\tau}} E\, d\tau = \text{a positive real constant}, \qquad \langle \dot{E} \rangle = \frac{1}{T}\int_{\hat{\tau}}^{T+\hat{\tau}} \dot{E}\, d\tau = 0, \tag{30}$$

$$\langle K \rangle = \frac{1}{T}\int_{\hat{\tau}}^{T+\hat{\tau}} K\, d\tau = \text{a positive real constant}, \qquad \langle \dot{K} \rangle = \frac{1}{T}\int_{\hat{\tau}}^{T+\hat{\tau}} \dot{K}\, d\tau = 0, \tag{31}$$

which can be quickly confirmed by the conditions in Equation (28).

2.5.4. Chaotic Motions (CMs)

CMs are considered as periodic motions with ***infinite period,*** and they have a non-positive time change rate of phase volume strain, so that the phase orbits are restricted in a finite domain, and the starting point of the orbit never coincides with a current orbit point. As a special periodical motion, its necessary condition in Equation (29) is valid, and the necessary conditions of Lyapunov exponents are satisfied, so that the chaotic orbits could appear. The sufficient conditions for POs in Equations (30) and (31) now take the following forms:

$$\langle E\rangle = \lim_{T\to\infty}\frac{1}{T}\int_{\hat{\tau}}^{T+\hat{\tau}} E\,d\tau = \text{a positive real constat}, \qquad \langle \dot{E}\rangle = \lim_{T\to\infty}\frac{1}{T}\int_{\hat{\tau}}^{T+\hat{\tau}} \dot{E}\,d\tau = 0, \tag{32}$$

$$\langle K\rangle = \lim_{T\to\infty}\frac{1}{T}\int_{\hat{\tau}}^{T+\hat{\tau}} K\,d\tau = \text{a positive real constat}, \qquad \langle \dot{K}\rangle = \lim_{T\to\infty}\frac{1}{T}\int_{\hat{\tau}}^{T+\hat{\tau}} \dot{K}\,d\tau = 0, \tag{33}$$

due to its period being infinite. As we mentioned in the Introduction, these criteria have been very effective in examining the reported chaotic phenomena [30,32]: the Van Der Pol Oscillator [38,39], Duffing's system [40], SD oscillator [41,42], Lorenz system [43,44], and Rössler oscillator [45].

3. Energy-Flow Investigations

3.1. Linear System

3.1.1. Theoretical Solution

When ε and ω are constants, Equation (1) becomes

$$\ddot{x} + 2\varepsilon\dot{x} + \omega^2 x = \widetilde{F}\cos\widetilde{\omega}\,\tau, \tag{34}$$

with its energy conservation equation

$$\frac{d}{d\tau}\left(\frac{\dot{x}^2}{2} + \frac{\omega^2 x^2}{2}\right) + 2\varepsilon\dot{x}^2 = \widetilde{F}\,\dot{x}\cos\widetilde{\omega}\,\tau. \tag{35}$$

The general solution of Equation (34) is a summation of the solution $x(a,b,\overline{\omega},\tau)$ of a non-forced system and a forced solution. The solution of a non-forced system can be obtained as

$$x(a,b,\overline{\omega},\tau) = ae^{r_1\tau} + be^{r_2\tau}, \quad \dot{x}(a,b,\overline{\omega},\tau) = ar_1e^{r_1\tau} + br_2e^{r_2\tau}, \tag{36}$$

$$r_{1,2} = \frac{-2\varepsilon \mp \sqrt{4\varepsilon^2 - 4\omega^2}}{2} = -\varepsilon \mp \sqrt{\varepsilon^2 - \omega^2}.$$

We are only interested in the oscillating case, $\omega^2 - \varepsilon^2 > 0$, $\varepsilon > 0$, for which Equation (36) can be rewritten as

$$x(a,b,\overline{\omega},\tau) = e^{-\varepsilon\tau}(a\sin\overline{\omega}\tau + b\cos\overline{\omega}\tau), \qquad \overline{\omega} = \sqrt{\omega^2 - \varepsilon^2}. \tag{37}$$

$$\dot{x}(a,b,\overline{\omega},\tau) = e^{-\varepsilon\tau}\overline{\omega}(a\cos\overline{\omega}\tau - b\sin\overline{\omega}\tau) - \varepsilon e^{-\varepsilon\tau}(a\sin\overline{\omega}\tau + b\cos\overline{\omega}\tau).$$

The general solution is

$$x = x(a,b,\overline{\omega},\tau) + \mathrm{Re}\left\{\frac{\widetilde{F}}{\omega^2 - 2\mathrm{i}\varepsilon\widetilde{\omega} - \widetilde{\omega}^2}e^{-\mathrm{i}\widetilde{\omega}\tau}\right\}, \quad \dot{x} = \dot{x}(a,b,\overline{\omega},\tau) + \mathrm{Re}\left\{\frac{-\mathrm{i}\widetilde{\omega}\widetilde{F}}{\omega^2 - 2\mathrm{i}\varepsilon\widetilde{\omega} - \widetilde{\omega}^2}e^{-\mathrm{i}\widetilde{\omega}\tau}\right\}, \tag{38}$$

of which the second term is the real part of the complex solution of forced vibration. Here, a and b are determined by the initial condition (x_0, p_0) at $\tau = 0$. From Equations (36) and (38), it follows

$$x_0 = b + \frac{(\omega^2 - \widetilde{\omega}^2)\widetilde{F}}{(\omega^2 - \widetilde{\omega}^2)^2 + 4\varepsilon^2\widetilde{\omega}^2}, \qquad b = x_0 - \frac{(\omega^2 - \widetilde{\omega}^2)\widetilde{F}}{(\omega^2 - \widetilde{\omega}^2)^2 + 4\varepsilon^2\widetilde{\omega}^2}, \tag{39}$$

$$p_0 = \overline{\omega}a - \varepsilon b + \frac{2\varepsilon\widetilde{\omega}^2\widetilde{F}}{(\omega^2 - \widetilde{\omega}^2)^2 + 4\varepsilon^2\widetilde{\omega}^2}, \quad a = \frac{1}{\overline{\omega}}\left\{ p_0 + \varepsilon x_0 - \frac{\varepsilon[(\omega^2 - \widetilde{\omega}^2) + 2\widetilde{\omega}^2]\widetilde{F}}{(\omega^2 - \widetilde{\omega}^2)^2 + 4\varepsilon^2\widetilde{\omega}^2} \right\}.$$

3.1.2. Energy Flow Variables and Matrices

The EFM, SM, EFE and EFCF for a linear system are

$$\boldsymbol{E} = \frac{1}{2}\begin{bmatrix} 0 & 1-\omega^2 \\ 1-\omega^2 & -4\varepsilon \end{bmatrix} = \text{constant}, \quad \boldsymbol{U} = \frac{1}{2}\begin{bmatrix} 0 & 1+\omega^2 \\ -1-\omega^2 & 0 \end{bmatrix} = \text{constant}, \tag{40}$$

$$\dot{E} = \begin{bmatrix} x & p \end{bmatrix}\begin{bmatrix} 0 & 1 \\ -\omega^2 & -2\varepsilon \end{bmatrix}\begin{bmatrix} x \\ p \end{bmatrix} + \begin{bmatrix} x & p \end{bmatrix}\begin{bmatrix} 0 \\ \widetilde{F}\cos\widetilde{\omega}\,\tau \end{bmatrix} \tag{41}$$

$$= \left(1-\omega^2\right)px - 2\varepsilon p^2 + pF = \left(1-\omega^2\right)\frac{d}{d\tau}\left(\frac{x^2}{2}\right) - 2\varepsilon p^2 + p\widetilde{F}\cos\widetilde{\omega}\,\tau,$$

$$\dot{K} = \begin{bmatrix} \dot{x} & \dot{p} \end{bmatrix}\boldsymbol{E}\begin{bmatrix} \dot{x} \\ \dot{p} \end{bmatrix} - \dot{p}\widetilde{\omega}\,\widetilde{F}\sin\widetilde{\omega}\,\tau = \left(1-\omega^2\right)\frac{d}{d\tau}\left(\frac{p^2}{2}\right) - 2\varepsilon\dot{p}^2 - \dot{p}\widetilde{\omega}\,\widetilde{F}\sin\widetilde{\omega}\,\tau, \tag{42}$$

$$\dot{E} = \lambda_1\eta_1^2 + \lambda_2\eta_2^2, \quad \lambda_{1,2} = \varepsilon\left\{ -1 \mp \sqrt{1 + \left(\frac{1-\omega^2}{2\varepsilon}\right)^2} \right\}, \quad \lambda_1 < 0, \quad \lambda_2 > 0, \tag{43}$$

$$\dot{v} = \lambda_1 + \lambda_2 = -2\varepsilon. \tag{44}$$

3.1.3. Chaotic Motions of Non-Damped Forced Vibrations ($\varepsilon = 0, \widetilde{F} \neq 0$)

Equations (37)–(39) give the theoretical solution of forced vibrations of a non-damping system as

$$x = \frac{p_0}{\omega}\sin\omega\tau + x_0\cos\omega\tau + \frac{\widetilde{F}}{\omega^2 - \widetilde{\omega}^2}(\cos\widetilde{\omega}\tau - \cos\omega\tau), \tag{45}$$

$$p = \dot{x} = p_0\cos\omega\tau - x_0\omega\sin\omega\tau - \frac{\widetilde{F}}{\omega^2 - \widetilde{\omega}^2}\left(\widetilde{\omega}\sin\widetilde{\omega}\tau - \omega\sin\omega\tau\right). \tag{46}$$

Considering an example with the initial conditions ($x_0 = 1, p_0 = 0$) and $\widetilde{F} = 1$, it takes as

$$x = \cos\omega\tau + \frac{1}{\omega^2 - \widetilde{\omega}^2}\left(\cos\widetilde{\omega}\tau - \cos\omega\tau\right), \qquad p = -\omega\sin\omega\tau - \frac{1}{\omega^2 - \widetilde{\omega}^2}(\widetilde{\omega}\sin\widetilde{\omega}\tau - \omega\sin\omega\tau). \tag{47}$$

It is important to mention that the general solution in Equation (47) consists of two oscillations with different frequencies. Due to no damping, the free vibration caused by initial conditions cannot be damped.

The EFE in Equations (41) and (42) becomes

$$\dot{E} = \left(1-\omega^2\right)\frac{d}{d\tau}\left(\frac{x^2}{2}\right) + p\,\widetilde{F}\cos\widetilde{\omega}\tau, \qquad \dot{K} = \left(1-\omega^2\right)\frac{d}{d\tau}\left(\frac{p^2}{2}\right) - \dot{p}\widetilde{\omega}\,\widetilde{F}\sin\widetilde{\omega}\tau. \tag{48}$$

For an average time $\overline{T}$, the TAEFs are

$$\langle \dot{E} \rangle = \frac{1}{\overline{T}} \int_0^{\overline{T}} \left\{ \left(1-\omega^2\right) \frac{d}{d\tau} \left(\frac{x^2}{2}\right) + p\, \widetilde{F} \cos\widetilde{\omega}\tau \right\} d\tau, \quad \langle \dot{K} \rangle = \frac{1}{\overline{T}} \int_0^{\overline{T}} \left\{ \left(1-\omega^2\right) \frac{d}{d\tau} \left(\frac{p^2}{2}\right) - \dot{p}\widetilde{\omega}\, \widetilde{F} \sin\widetilde{\omega}\tau \right\} d\tau. \tag{49}$$

which are affected by the periods $T/\pi = 2/\omega$ and $\widetilde{T}/\pi = 2/\widetilde{\omega}$ as follows.

A. Periods $T/\pi = 2/\omega$ and $\widetilde{T}/\pi = 2/\widetilde{\omega}$ have their ***rational*** least common multiple (LCM), so that the integrands in the integrations Equation (49) are the periodic functions of period $\pi *$ LCM, and we have TAEF

$$\langle \dot{E} \rangle = 0 = \langle \dot{K} \rangle, \tag{50}$$

implying the motion is periodic.

B. Periods $T/\pi = 2/\omega$ and $\widetilde{T}/\pi = 1$ do not have their LCM, for example, a rational frequency and an irrational one, we cannot find a common period, making the integration Equation (49) zero.

Table 1 lists the parameters of 3 examples, which have been numerically simulated with the results shown in Figure 4.

Table 1. The parameters of the 2 cases in Figure 4 with the related LCMs.

Cases	ω	$T/\pi = 2/\omega$	$\widetilde{\omega}$	$\widetilde{T}/\pi = 2/\widetilde{\omega}$	LCM	$\pi *$LCM
(I)	1	2	2	1	2	2π
(II)	1	2	$\sqrt{2}$	$2/\sqrt{2}$	No	No
(III)	1	2	$\sqrt{3}$	$2/\sqrt{3}$	No	No

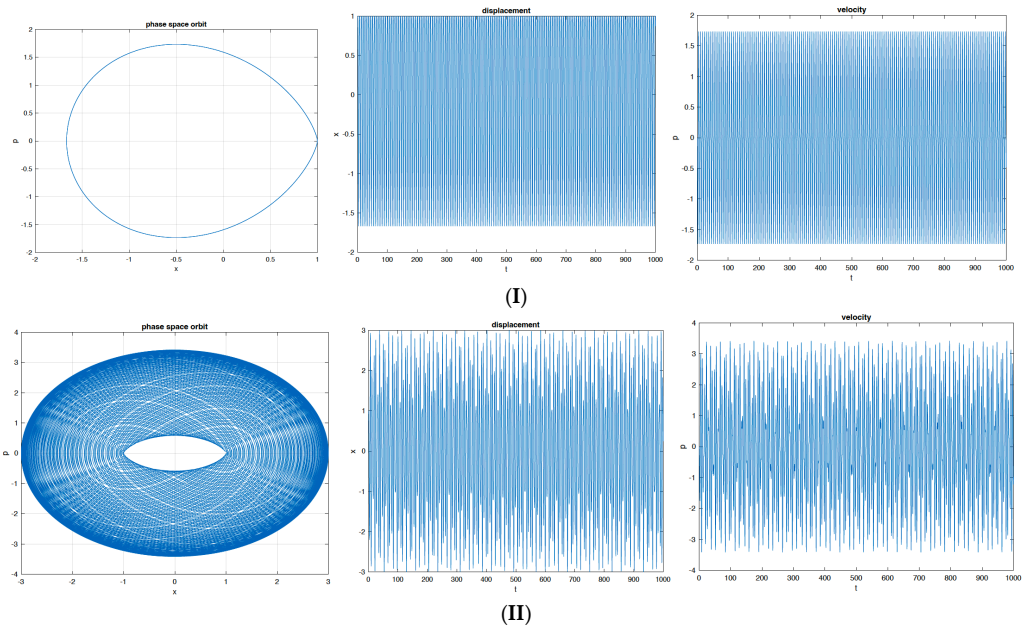
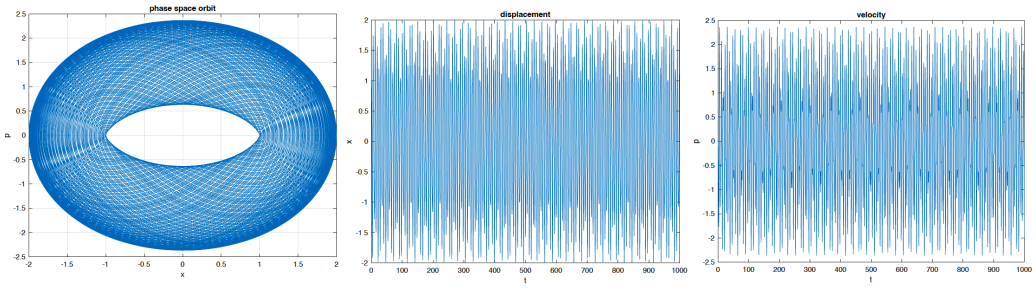


Figure 4. *Cont.*

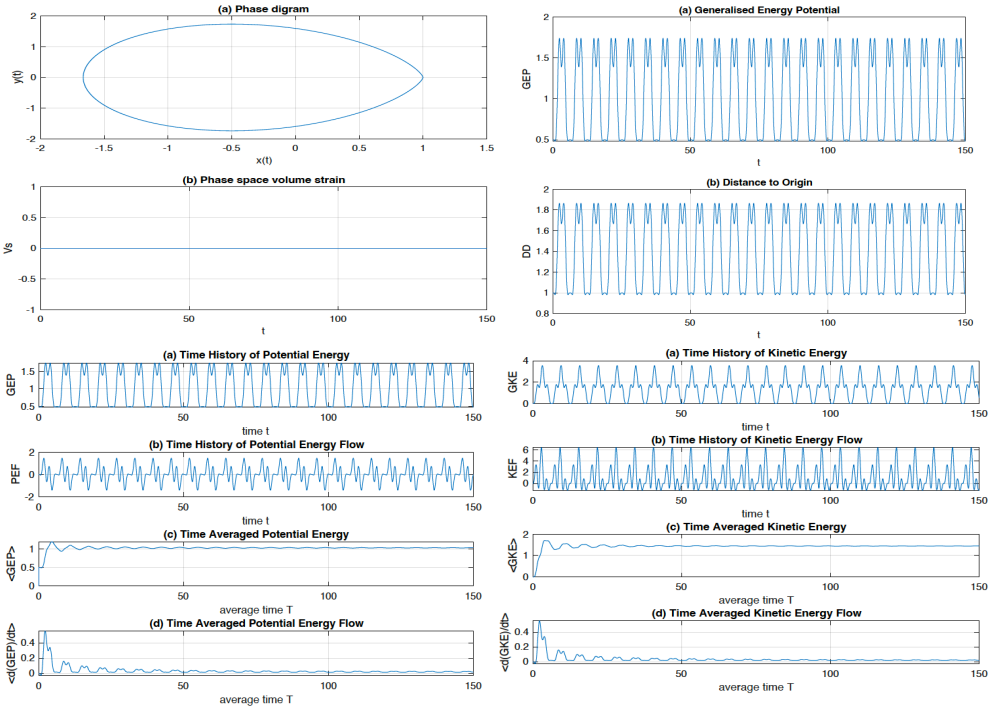


(**III**)

Figure 4. Time histories and phase space orbits of a linear forced system ($\varepsilon = 0,\ \ x_0 = 1,\ p_0 = 0$) from the theoretical solution in Equation (55) for the three cases: (**I**) $\omega = 1, \widetilde{\omega} = 2$; (**II**) $\omega = 1, \widetilde{\omega} = \sqrt{2}$; (**III**) $\omega = 1, \widetilde{\omega} = \sqrt{3}$.

Based on the theoretical solutions in Equation (47), we can avoid any numerical errors to draw the time histories and the orbits in the phase space of a 1-DOF no-damping forced system in Figure 4 for 3 cases: (I) $\omega = 1, \widetilde{\omega} = 2$; (II) $\omega = 1, \widetilde{\omega} = \sqrt{2}$; (III) $\omega = 1, \widetilde{\omega} = 3$. As indicated in Table 1, Case (I) with a rational LCM, the orbit in the phase space is a closed curve and the motions are periodic, while for Cases (II, III), no LCM, the orbits are not closed curves, where the phase points move between two circles, and the motions are chaotic. The time histories of displacements and velocities for three Cases, respectively, consist of two components, from which you can clearly see that Case (I) has a common period showing horizontal envelope lines; while Cases (II) and (III) do not have common periods, so they do not show these common envelopes.

Figure 5 provides the corresponding energy-flow diagrams obtained by energy flow numerical simulations, from which we can see: Case (I) GPE of composed motion is a single closed curve due to its LCM, the time averaged energies and flows by the common period, respectively, tend to positive constants and zeros, while Cases (II, III) show chaotic orbits in phase space due to not LCMs, the time averaged energies and flows are, respectively, tend to constant positive numbers and zeros when the average time is increasing.



(**I**)

Figure 5. *Cont.*

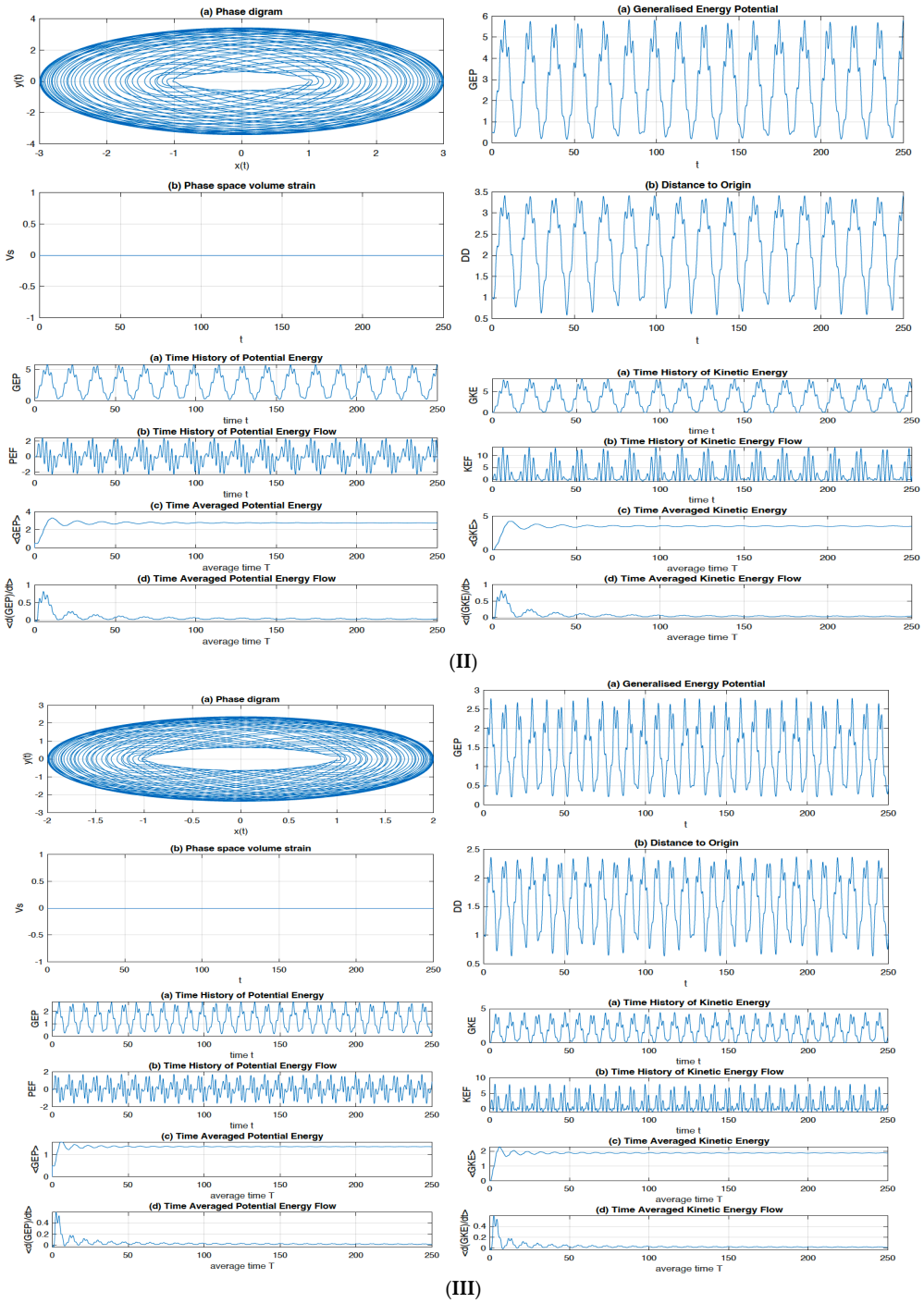


Figure 5. (**I**) The phase diagram, the GPE, GKE and their TAEFs of forced/free vibrations for a linear 1-DOF system ($\varepsilon = 0,\ \ x_0 = 1,\ p_0 = 0, \omega = 1, \widetilde{\omega} = 2$). (**II**) The phase diagram, the GPE, GKE and their TAEFs of forced/free vibrations for a linear 1-DOF system ($\varepsilon = 0,\ \ x_0 = 1,\ p_0 = 0,$ $\omega = 1, \widetilde{\omega} = \sqrt{2}$). (**III**) The phase diagram, the GPE, GKE and their TAEFs of forced/free vibrations for a linear 1-DOF system ($\varepsilon = 0,\ \ x_0 = 1,\ p_0 = 0, \omega = 1, \widetilde{\omega} = \sqrt{3}$).

For the motions in Figures 4(II,III) and 5(II,III), the phase points starting from their initial positions are restricted in the finite domains because the phase space volume strain (Vs) is zero and never come back to their starting points to construct closed curves. Also, Figure 5(II,III) shows that the TAEF tend to zero when the averaged time cap T bar goes to infinity; therefore, they are the periodic motions with infinite periods, the chaotic motions based on EFT. As a result of this, *we may say that the LCM of two periods with no finite rational*

LCM is ∞*, which is why chaotic motions are considered as periodical motions with infinite period*. The above mathematical and numerical demonstrations are concluded as follows.

Chaotic motion in a linear non-damping system: *For a 1-DOF linear non-damping forced system with its natural frequency* ω *and the excitation force frequency* $\widetilde{\omega}$*, if there exists a rational LCM for the two periods, the composed motion, consisting of the free motion due to initial conditions and the forced one caused by the excitation, is a periodical motion in the period* $\pi *$ LCM*; if there is no LCM of these two numbers, the composed motion is chaotic.*

3.2. Nonlinear Systems

The following 1-DOF NDS with nonlinear stiffness/damping are investigated by EFT to reveal their dynamic characteristics.

3.2.1. Nonlinear Stiffness

We consider a system with a nonlinear stiffness $\omega^2(x) = \alpha + \beta x + \gamma x^2$, where α, β, γ are real numbers. The parameters affect the dynamic behaviours of the system as follows.

- $\omega^2(x) < 0 : \ \gamma > o,\ \beta^2 - 4\alpha\gamma > 0$, or $\gamma < o,\ \beta^2 - 4\alpha\gamma < 0$. Nonlinear stiffness is variable negative, so that the system is unstable and the motion is divergent if there is no damping or excitation force. Figure 6(I,II) show two cases: (I) $\omega^2(x) = -2 + x + x^2,\ -2 < x < 1$, (II) $\omega^2(x) = -2 - x - x^2$.
- $\omega^2(x) > 0 : \ \gamma < o,\ \beta^2 - 4\alpha\gamma > 0$, or $\gamma > o,\ \beta^2 - 4\alpha\gamma < 0$. Nonlinear stiffness is variable positive, so that the system is stable, and the motions could be periodic and chaotic depending on the damping and excitation force. Figure 6(III,IV) show two cases where (III) $\omega^2(x) = 2 - x - x^2,\ -2 < x < 1$, (IV) $\omega^2(x) = 2 + \dot{x} + \dot{x}^2$.

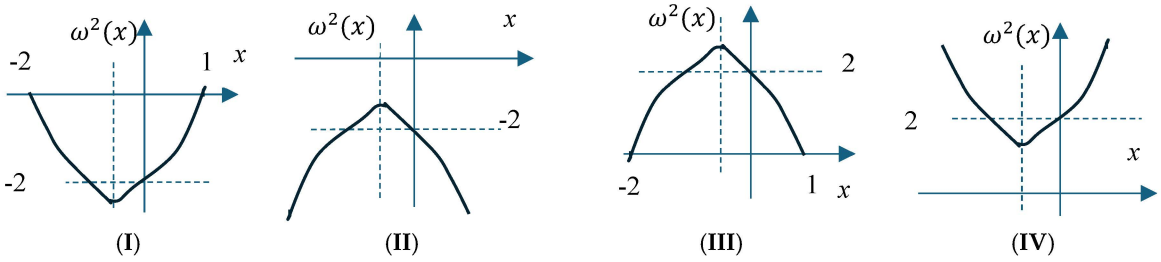


Figure 6. The nonlinear stiffness functions: $\omega^2(x) < 0$, **(I)** $\omega^2(x) = -2 + x + x^2,\ -2 < x < 1$, **(II)** $\omega^2(x) = -2 - x - x^2$; $\omega^2(x) > 0$, **(III)** $\omega^2(x) = 2 - x - x^2,\ -2 < x < 1$, **(IV)** $\omega^2(x) = 2 + \dot{x} + \dot{x}^2$.

We numerically investigate the cases with the parameters $\alpha = -1,\ \beta = 0,\ \gamma = 1,\ \widetilde{\omega} = 1,\ \widetilde{F} = 0.3$ and $2\varepsilon = 0.15,\ 0.22$, which construct the Duffing's equations investigated by Mood & Homes (1979) [40] who reported the periodical solution in the damping 0.22, and the chaotic motion in the damping of 0.15.

The state equation and EFE of the system ($\beta = 0$) are

$$\begin{bmatrix} \dot{x} \\ \dot{p} \end{bmatrix} = \begin{bmatrix} 0 & 1 \\ -\omega^2(x) & -2\varepsilon \end{bmatrix} \begin{bmatrix} x \\ p \end{bmatrix} + \begin{bmatrix} 0 \\ \widetilde{F}\cos\widetilde{\omega}\tau \end{bmatrix}, \qquad \dot{v} = -2\varepsilon, \tag{51}$$

$$\dot{E} = \left[1 - \omega^2(x)\right] xp - 2\varepsilon p^2 + p\,\widetilde{F}\cos\widetilde{\omega}\tau, \tag{52}$$

$$\dot{K} = \left[1 - \omega^2(x)\right] p\dot{p} - 2\varepsilon\dot{p}^2 - \dot{p}\widetilde{\omega}\,\widetilde{F}\sin\widetilde{\omega}\tau. \tag{53}$$

Case I: Free vibration ($\varepsilon = 0 = \widetilde{F},\ \omega > 0$)

Equations (52) and (53) become

$$\dot{E} = \left[1 - \omega^2(x)\right] xp = \left[1 - \omega^2(x)\right] x\frac{dx}{d\tau}, \tag{54}$$

$$\dot{K} = \left[1 - \omega^2(x)\right] p\dot{p} = \left[1 - \omega^2(x)\right] \frac{d}{d\tau}(\frac{p^2}{2}). \tag{55}$$

Integrating Equation (54) with respect to time along a curve from $x = 0$, and noting the definition of GPE, we obtain

$$E = \int_0^x \left[1 - \omega^2(x)\right] x dx = \frac{1-\alpha}{2}x^2 - \frac{\gamma}{4}x^4 = \frac{1}{2}(x^2 + p^2), \tag{56}$$

$$\langle \dot{E} \rangle = \frac{1}{T}\oint \left[1 - \omega^2(x)\right] x dx = 0, \tag{57}$$

from which it follows

$$\frac{p^2}{2} = -\frac{\alpha}{2}x^2 - \frac{\gamma}{4}x^4, \qquad \frac{d}{dt}\left(\frac{p^2}{2}\right) = -\omega^2(x)x\frac{dx}{d\tau}. \tag{58}$$

Substituting Equation (58) into Equation (55) and then integrating it along the closed curve, we obtain

$$\langle \dot{K} \rangle = \frac{1}{T}\oint \left[\omega^2(x) - 1\right] \omega^2(x) x dx = 0. \tag{59}$$

The conditions for periodical motion are satisfied at each position x, so that the motion at x is a periodic motion of frequency $\omega(x)$. As given in [58], many approximation approaches, such as the perturbed simple harmonic one, homotopy analysis, and Hamiltonian bounded methods, have been reported to obtain the corresponding approximated solution restricted in a small area, which may show a local approximated periodical behaviour. To confirm it is a real periodic one, its phase space diagram must be a closed single curve. Generally, due to x being a continuous variable during the motion, for large, long-time motion, the frequencies $\omega(x)$ with its variable periods, as indicated by the theoretical solution by Jacobi's elliptic functions [58], include many different components, which normally cannot have a finite LCM, or have an infinite LCM, so that no common finite period for all frequencies and the phase space diagram shows chaotic according to EFT.

Case II: Forced vibrations of a no-damping system ($\varepsilon = 0,\ F \neq 0,\ \omega > 0$)

In this case, EFEs are obtained by Equations (52) and (53) with $\varepsilon = 0$, of which TAEFs are

$$\langle \dot{E} \rangle = \frac{1}{\overline{T}}\int_0^{\overline{T}} \left\{ \left[1 - \omega^2(x)\right] \frac{d}{d\tau}\left(\frac{x^2}{2}\right) + p\widetilde{F}\cos\widetilde{\omega}\tau \right\} d\tau = \frac{1}{\overline{T}}\left\{ \left[\frac{x^2}{2} - W(x)\right]\Big|_0^{\overline{T}} + \int_0^{\overline{T}} p\widetilde{F}\cos\widetilde{\omega}\tau d\tau \right\}, \tag{60}$$

$$\langle \dot{K} \rangle = \frac{1}{\overline{T}}\int_0^{\overline{T}} \left\{ \left[1 - \omega^2(x)\right] \frac{d}{d\tau}\left(\frac{p^2}{2}\right) - \dot{p}\widetilde{\omega}\widetilde{F}\sin\widetilde{\omega}\tau \right\} d\tau, \qquad W(x) = \int \left[\omega^2(x)\right] \frac{d}{d\tau}\left(\frac{x^2}{2}\right). \tag{61}$$

The nonlinear stiffness $\omega^2(x) = \alpha + \gamma x^2$ is imaged as the variable natural frequency $\omega(x)$ of period $T(x)$, the functions of the position x, so that for a fixed force frequency $\widetilde{\omega}$ of period $\widetilde{T}$, it is unable to find an LCM for the variable $T(x)$ with $\widetilde{T}$, and therefore the resultant motion is chaotic.

Figure 7 shows the numerical results of three cases for the systems with the nonlinear stiffness terms γx^2, in which Case (I) is a free vibration with no excitation force, while Cases (II) and (III) are forced vibrations with different values of the parameter γ. As we have predicted above, Cases (I, II, III) show the motion orbits and TAEF curves satisfying

the rules of chaotic motions, so that the motions are chaotic. To summarise the theoretical discussion and numerical results, we may conclude the following chaotic motion.

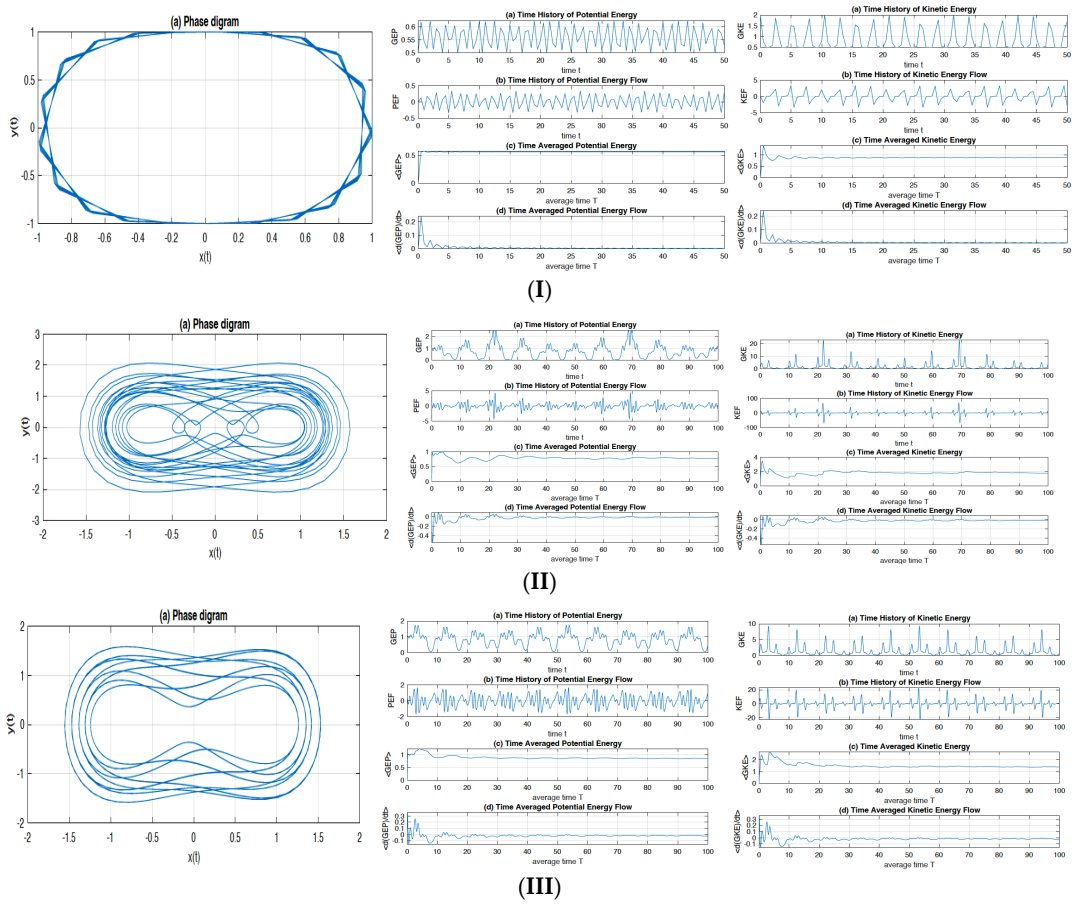


Figure 7. The energy-flow diagrams of forced and free vibrations of nonlinear non-damping systems ($\varepsilon = 0,\ x_0 = 1,\ p_0 = 0$) : (**I**) free vibration $\left(\gamma = 2,\ \overline{F} = 0\right)$; (**II**) forced vibration $\left(\gamma = 2,\ \overline{F} = 1, \widetilde{\omega} = 1\right)$; (**III**) forced vibration $\left(\gamma = \sqrt{2},\ \overline{F} = 1, \widetilde{\omega} = 1\right)$.

Chaotic motion in non-damping systems with nonlinear stiffness: *For a 1-DOF nonlinear non-damping forced system with the nonlinear stiffness in the form of* $\gamma x^2,\ (\gamma > 0)$, *both the free motion by initial conditions and the composed motions with the forced one caused by the excitation are chaotic, since the nonlinear stiffness, as a continuous function of displacement* x, *generates continuous 'imaged natural frequencies' unable to have their LCM as well as the LCM with the excitation frequency.*

Case III: Forced vibrations of a damping system $\left(\varepsilon > 0,\ \widetilde{F} \neq 0\right)$

For the forced vibrations of the damping system, from Equations (51)–(53), TAEFs are

$$\begin{aligned}\langle \dot{E} \rangle &= \frac{1}{\overline{T}} \int_0^{\overline{T}} \left\{ \left[1 - \omega^2(x)\right] \frac{dx^2}{2d\tau} - 2\varepsilon p^2 + p\widetilde{F} \cos\widetilde{\omega}\tau \right\} d\tau \\ &= \frac{1}{\overline{T}} \left\{ \left[\frac{x^2}{2} - W(x) \right] \Big|_0^{\overline{T}} + \int_0^{\overline{T}} \left(-2\varepsilon p^2 + p\widetilde{F} \cos\widetilde{\omega}\tau \right) d\tau \right\},\end{aligned} \tag{62}$$

$$\langle \dot{K} \rangle = \frac{1}{\overline{T}} \int_0^{\overline{T}} \left\{ \left[1 - \omega^2(x)\right] \frac{d}{d\tau} \left(\frac{p^2}{2} \right) - 2\varepsilon \dot{p}^2 - \dot{p}\widetilde{\omega}\widetilde{F} \sin\widetilde{\omega}\tau \right\} d\tau \tag{63}$$

As we have learnt that for linear systems, the damping will dampen the free vibration components to zero as time increases, resulting in a periodical forced vibration with the force frequency. However, for nonlinear systems, this is not true, since the frequencies of forced vibrations are not unique. Therefore, although the free vibrations in nonlinear

systems are damped to zero, the remaining forced vibrations have many frequencies with no LCM, resulting in the composed motion exhibiting chaotic characteristics. Figure 8 shows the numerical results of two cases, where (I) is a free vibration and it gradually decreases to ZEFS due to the damping, while (II) is a forced case, in which the free vibration component is reduced, but the forced vibration components show chaotic motions. This result can be concluded as the following chaotic motion.

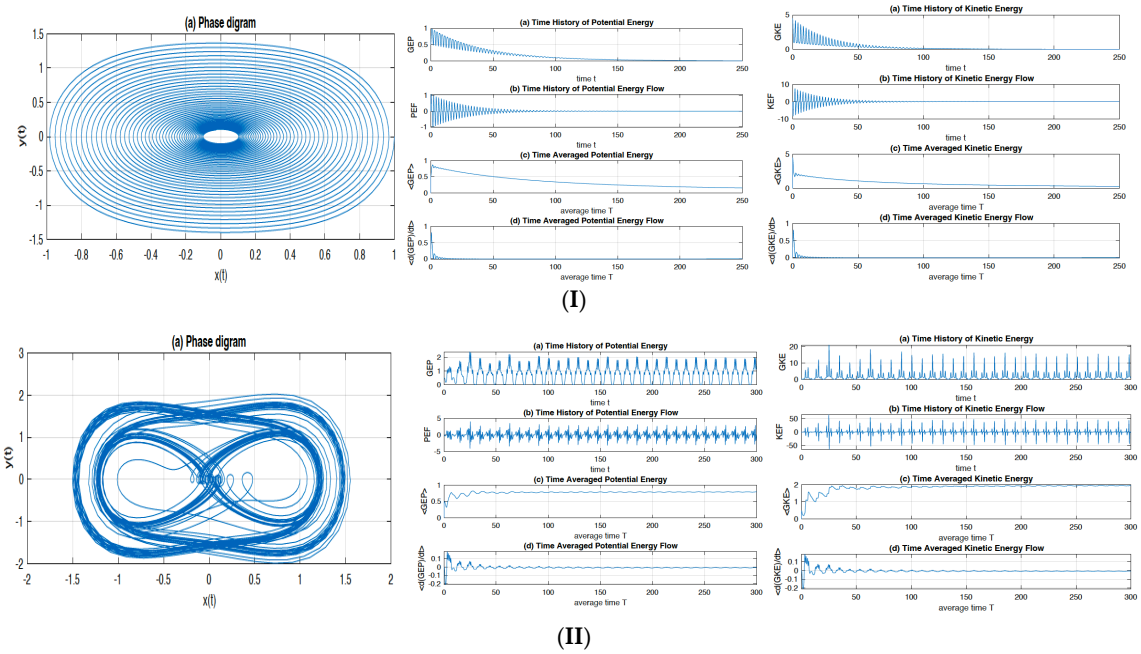


Figure 8. The energy-flow diagrams of free and forced vibration of a nonlinear damping system ($\varepsilon = 0.01,\ x_0 = 1,\ p_0 = 0$) : (**I**) free vibration $(\gamma = 2,\ \overline{F} = 0)$; (**II**) forced vibration $\left(\gamma = 2,\ \widetilde{F} = 1, \widetilde{\omega} = 1\right)$.

Chaotic motion in a damping system with nonlinear stiffness: *For a 1-DOF nonlinear damping forced system with the nonlinear stiffness in the form of* γx^2, $(\gamma > 0)$, *the free motion by initial condition gradually tends to zero due to damping, but the forced vibration caused by the excitation with a given frequency consists of different frequency components showing chaotic motion characteristics.*

3.2.2. Nonlinear Damping

We consider a system with a nonlinear damping $2\varepsilon(\dot{x}) = 2\varepsilon + b\dot{x} + c\dot{x}^2$, where ε, b, c are real numbers. For free vibrations ($\widetilde{F} = 0,\ \omega > 0$), the solutions can be discussed from Equation (37) with the nonlinear damping $\varepsilon(\dot{x})$. For different values of the parameter ε, the corresponding free vibrations have the following characteristics.

- $0 < |\varepsilon| < \omega$, $x = Ae^{-\varepsilon\tau}e^{-i\overline{\omega}\tau} + Be^{-\varepsilon\tau}e^{i\overline{\omega}\tau}$, $\overline{\omega} = \sqrt{\omega^2 - \varepsilon^2}$, the frequency of free vibration, which is less than the natural frequency ω. The motion is an amplitude-decreasing oscillation when positive damping $\varepsilon > 0$, but an amplitude increasing oscillation if $\varepsilon < 0$.
- $|\varepsilon| \geq \omega$, $r_{1,2}$ are two negative real numbers if $\varepsilon > 0$, the displacement x decreases with no oscillation; while when $\varepsilon < 0$, $r_{1,2}$ are positive real numbers, and the displacement increases.

Non-forced nonlinear damping system ($\widetilde{F} = 0,\ \omega > 0$)

For nonlinear damping cases, the nonlinear damping term $2\varepsilon(\dot{x})$ plays the role of 2ε for the linear system, the dynamic equation and EFEs are

$$\ddot{x} + 2\varepsilon(\dot{x})\dot{x} + \omega^2 x = 0, \tag{64}$$

$$\dot{E} = \left[1-\omega^2\right]\frac{d}{d\tau}(\frac{x^2}{2}) - 2\varepsilon(p)p^2, \qquad \langle\dot{E}\rangle = \frac{1}{\overline{T}}\oint\left\{\left[1-\omega^2\right]\frac{d}{d\tau}(\frac{x^2}{2}) - 2\varepsilon(p)p^2\right\}d\tau, \tag{65}$$

$$\dot{K} = \left[1-\omega^2\right]\frac{d}{d\tau}(\frac{p^2}{2}) - 2\varepsilon(p)\dot{p}^2, \qquad \langle\dot{K}\rangle = \frac{1}{\overline{T}}\oint\left\{\left[1-\omega^2\right]\frac{d}{d\tau}(\frac{p^2}{2}) - 2\varepsilon(p)p^2\right\}d\tau, \tag{66}$$

and the energy conservation equation becomes

$$\frac{1}{2}\left(x_0^2+p_0^2\right) - \frac{1}{2}\left(x^2+p^2\right) = \int_0^T 2\varepsilon(p)p^2 d\tau, \qquad E_0 - E = \int_0^T 2\varepsilon(p)p^2 d\tau. \tag{67}$$

The dissipating or absorbing energy of the system depends on the negative or positive values of the integration on the right-hand side of Equation (67). Since the damping $2\varepsilon(\dot{x})$ is the nonlinear function of $\dot{x}$, so that for different time, the free vibration frequency $\overline{\omega}(\dot{x}) = \sqrt{\left|\varepsilon(\dot{x})^2 - \omega^2\right|}$ is also a function of time affecting the dynamic characteristics. As an example, we consider $\omega = 1$, $c = \pm 1$, $b = 1$ to discuss it, for which Equation (65) becomes

$$\dot{E} = -2\varepsilon(p)p^2 : \begin{cases} > 0, & \varepsilon(p) < 0, \quad -1 < p < 0, \\ = 0, & \varepsilon(p) = 0, \quad p = -1, \\ < 0, & \varepsilon(p) > 0, \quad p < -1, \end{cases} \tag{68}$$

which implies that $\omega = 1$ and $p = -1$ defines a ZEFS, which is discussed in the following two cases.

(a) $\left(\varepsilon(\dot{x})^2 < \omega^2\right) : 0 < \left|\varepsilon(\dot{x})\right| < 1$ and $0 < \left|2\varepsilon(\dot{x})\right| < 2$, we have the following two cases shown in Figure 9(I,II), where (I) for $2\varepsilon(\dot{x}) = -2 + \dot{x} + \dot{x}^2$, $\varepsilon(\dot{x}) < 0$; and (II) for $2\varepsilon(\dot{x}) = 2 - \dot{x} - \dot{x}^2, \varepsilon(\dot{x}) > 0$. Figure 10(I,II) shows the corresponding energy-flow diagrams, from which you can see that in Case (I), since the damping is negative, the amplitude $\left|\dot{x}\right|$ of oscillation increases from the initial position ($x_0 = 1, p_0 = 0, 2\varepsilon(\dot{x}) = -2$) locating inside of ZEFS towards the curve due to $\varepsilon(\dot{x}) < 0$ and $\dot{E} > 0$. When the amplitude of velocity reaches $\left|\dot{x}\right| \to |-2| = 2$, where is a turning point $2\varepsilon(\dot{x}) = 0$ corresponding ZEFS. After this point, it will be $2\varepsilon(\dot{x}) > 0$, the amplitude of velocity starts to decrease and $\dot{E} < 0$, the phase point returns to the curve, so that this curve is a stable limit circle as shown in Figure 10(I). Since the $\overline{\omega}(\dot{x}) = \sqrt{\left|\varepsilon(\dot{x})^2 - \omega^2\right|}$ it is continually changed with time; there is no LCM. The phase point along a not-repeating orbit oscillates around ZEFS. However, for Case in Figure 10(II), the damping is positive, the motion is damped from the initial point ($x_0 = 1, p_0 = 0$) until its static EP (0, 0) is shown in the figure. To conclude this dynamic characteristic, we have the following motion.

Non-repeating motion orbit towards a limit circle in NDS: *For a 1-DOF NDS governed by the equation*

$$\ddot{x} + 2\varepsilon(\dot{x})\dot{x} + x = 0, \quad 2\varepsilon(\dot{x}) = -2 + \dot{x} + \dot{x}^2, \quad \varepsilon(\dot{x}) < 0, \quad \varepsilon(\dot{x})^2 < 1, \tag{69}$$

The motion of free vibration caused by the initial conditions ($x_0 = 1, p_0 = 0$) *along a non-repeating orbit towards a zero energy-flow limit circle of* $\dot{E} = 0$, $p = -1$. *This type of orbit is due to the free vibration frequency* $\overline{\omega}(\dot{x}) = \sqrt{\left|\varepsilon(\dot{x})^2 - 1\right|}$ *is a continuous function of* $\dot{x}$, *so that is not their LCM.*

Here, it may be needed to mention that the above *ZEFS limit circle* numerically obtained just shows the prediction from the Poincare-Bendixson theorem [59,60], which says: the attractors for any smooth 2D-bounded continuous-time autonomous system are either a stable equilibrium or a *limit cycle*.

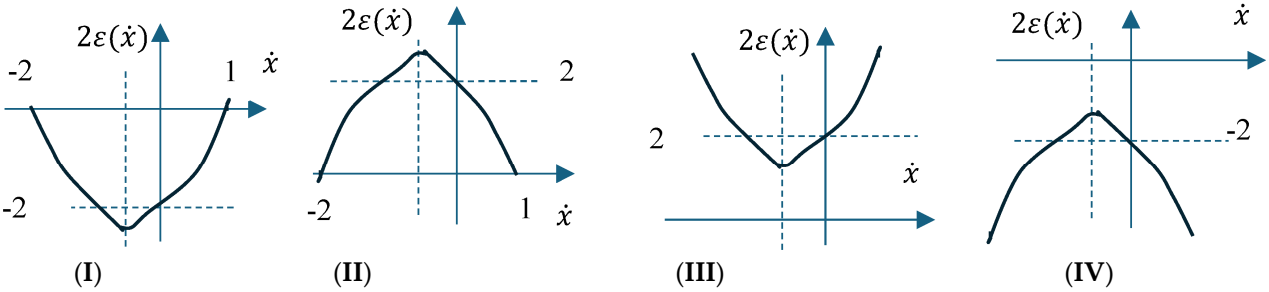


Figure 9. The nonlinear damping functions: for $0 < |2\varepsilon(\dot{x})| < 2$, **(I)** $2\varepsilon(\dot{x}) = -2 + \dot{x} + \dot{x}^2$, $\varepsilon(\dot{x}) < 0$; **(II)** $2\varepsilon(\dot{x}) = 2 - \dot{x} - \dot{x}^2$, $\varepsilon(\dot{x}) > 0$; and for $|2\varepsilon(\dot{x})| > 2$, **(III)** $2\varepsilon(\dot{x}) = 2 + \dot{x} + \dot{x}^2$, $\varepsilon(\dot{x}) > 0$; **(IV)** $2\varepsilon(\dot{x}) = -2 - \dot{x} - \dot{x}^2$, $\varepsilon(\dot{x}) < 0$.

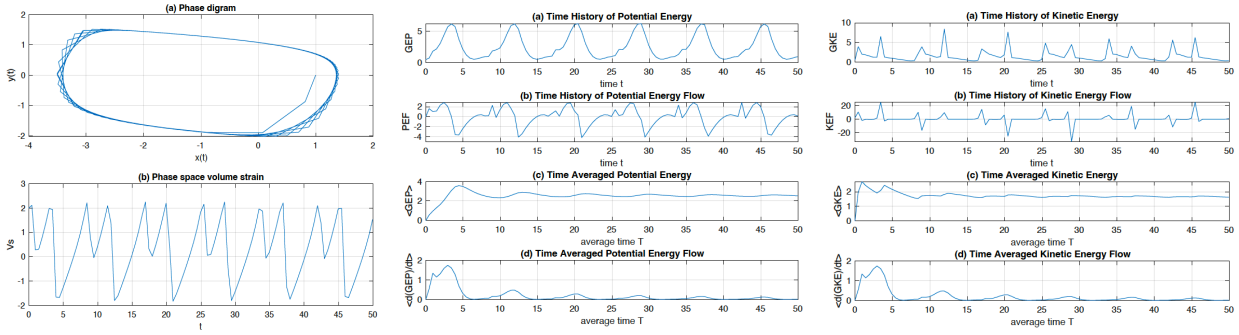
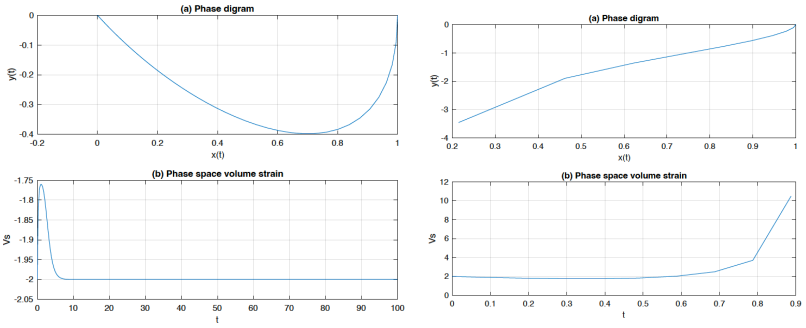


Figure 10. The energy-flow diagrams of the two nonlinear damping cases: **(I)** $2\varepsilon(\dot{x}) = -2 + \dot{x} + \dot{x}^2$, $\varepsilon(\dot{x}) < 0$; **(II)** $2\varepsilon(\dot{x}) = 2 - \dot{x} - \dot{x}^2$, $\varepsilon(\dot{x}) > 0$.

(b) $\left(\varepsilon(\dot{x})^2 > \omega^2\right)$: $|\varepsilon(\dot{x})| > 1$ with $|2\varepsilon(\dot{x})| > 2$, the two cases are shown in Figure 9(III,IV), where (III) for $2\varepsilon(\dot{x}) = 2 + \dot{x} + \dot{x}^2$, $\varepsilon(\dot{x}) > 0$; and (IV) for $2\varepsilon(\dot{x}) = -2 - \dot{x} - \dot{x}^2$, $\varepsilon(\dot{x}) < 0$. The corresponding energy-flow diagrams are shown in Figure 11, where (I) the curve shows a damped motion from the initial time to the origin due to positive damping, but (II) the curve is a divergence motion due to negative damping.



(I) **(II)**

Figure 11. The phase-space diagrams for the free motions of a nonlinear damping system: **(I)** $2\varepsilon(\dot{x}) = 2 + \dot{x} + \dot{x}^2, \varepsilon(\dot{x}) > 0$, **(II)** $2\varepsilon(\dot{x}) = -2 - \dot{x} - \dot{x}^2, \varepsilon(\dot{x}) < 0$.

4. Energy-Flow Behaviour of QPS and Its Extension to N-DOF Linear Systems

4.1. QPS

It has been realised that the investigated 1-DOF non-damping forced system satisfies the condition of QPS [61], that is, for a set of m positive frequencies ω_I and a set of non-zero integers c_I the following condition is valid

$$\sum_{I=1}^{m} c_I \omega_I \neq 0, \tag{70}$$

implying that these m positive frequencies are linearly rationally independent. In our words, there is no LCM of the periods of all frequencies of the system, i.e., the common period of the system is infinite. Therefore, for non-damping QPSs, their phase space orbits will be chaotic. We investigate a 2-DOF example as follows.

4.2. A 2-DOF Example

4.2.1. Governing Equation

The 2-DOF example is governed by the equation,

$$\begin{bmatrix} 1 & 0 \\ 0 & 1 \end{bmatrix} \begin{bmatrix} \ddot{x}_1 \\ \ddot{x}_2 \end{bmatrix} + \begin{bmatrix} 1 & -1 \\ -1 & 2 \end{bmatrix} \begin{bmatrix} x_1 \\ x_2 \end{bmatrix} = 0, \quad \begin{bmatrix} x_1 \\ x_2 \end{bmatrix}(0) = \begin{bmatrix} x_1 \\ x_2 \end{bmatrix}^*, \quad \begin{bmatrix} \dot{x}_1 \\ \dot{x}_2 \end{bmatrix}(0) = \begin{bmatrix} \dot{x}_1 \\ \dot{x}_2 \end{bmatrix}^*, \tag{71}$$

which is an equation of free vibrations caused by the initial conditions. It is not difficult to solve its natural frequencies and modes as

$$\omega_{1,2} = \pm\frac{3-\sqrt{5}}{2}, \quad \boldsymbol{\phi}_I = \frac{1}{a_I}\begin{bmatrix} 1 \\ 1-\omega_I \end{bmatrix}, \quad a_I = \sqrt{1+(1-\omega_I)^2}, \quad I = 1, 2, \tag{72}$$

satisfying the orthogonality relationships

$$\begin{bmatrix} \boldsymbol{\phi}_1^T \\ \boldsymbol{\phi}_2^T \end{bmatrix} \begin{bmatrix} 1 & 0 \\ 0 & 1 \end{bmatrix} \begin{bmatrix} \boldsymbol{\phi}_1 & \boldsymbol{\phi}_2 \end{bmatrix} = \begin{bmatrix} 1 & 0 \\ 0 & 1 \end{bmatrix}, \quad \begin{bmatrix} \boldsymbol{\phi}_1^T \\ \boldsymbol{\phi}_2^T \end{bmatrix} \begin{bmatrix} 1 & -1 \\ -1 & 2 \end{bmatrix} \begin{bmatrix} \boldsymbol{\phi}_1 & \boldsymbol{\phi}_2 \end{bmatrix} = \begin{bmatrix} \omega_1^2 & 0 \\ 0 & \omega_2^2 \end{bmatrix}. \tag{73}$$

For this system, Equation (70) is valid, i.e., for any two integers

$$\frac{3+\sqrt{5}}{2}c_1 + \frac{3-\sqrt{5}}{2}c_2 \neq 0, \tag{74}$$

implying there is not a common period (LCM) of the two periods of the system, so that it is a quasi-periodical system with its period being infinite.

4.2.2. EFE

Our aim is to investigate its energy flow characteristics from which to tackle its possible chaotic motion, so that we rewrite Equation (71) in its form in the phase space as

$$\begin{bmatrix}\dot{\boldsymbol{x}}\\ \dot{\boldsymbol{p}}\end{bmatrix}=\begin{bmatrix}0 & \boldsymbol{I}\\ -\boldsymbol{k} & 0\end{bmatrix}\begin{bmatrix}\boldsymbol{x}\\ \boldsymbol{p}\end{bmatrix},\qquad \boldsymbol{x}=\begin{bmatrix}x_1\\ x_2\end{bmatrix},\quad \boldsymbol{p}=\begin{bmatrix}\dot{x}_1\\ \dot{x}_2\end{bmatrix},\quad \boldsymbol{k}=\begin{bmatrix}1 & -1\\ -1 & 2\end{bmatrix},\quad \boldsymbol{I}=\begin{bmatrix}1 & 0\\ 0 & 1\end{bmatrix}. \tag{75}$$

The EFE of the system is

$$\dot{E}=\begin{bmatrix}\boldsymbol{x}^T & \boldsymbol{p}^T\end{bmatrix}\begin{bmatrix}0 & \boldsymbol{I}\\ -\boldsymbol{k} & 0\end{bmatrix}\begin{bmatrix}\boldsymbol{x}\\ \boldsymbol{p}\end{bmatrix}=\begin{bmatrix}\boldsymbol{x}^T & \boldsymbol{p}^T\end{bmatrix}(\boldsymbol{E}+\boldsymbol{U})\begin{bmatrix}\boldsymbol{x}\\ \boldsymbol{p}\end{bmatrix}=\begin{bmatrix}\boldsymbol{x}^T & \boldsymbol{p}^T\end{bmatrix}(\boldsymbol{E})\begin{bmatrix}\boldsymbol{x}\\ \boldsymbol{p}\end{bmatrix},\qquad E=\frac{1}{2}\begin{bmatrix}\boldsymbol{x}^T & \boldsymbol{p}^T\end{bmatrix}\begin{bmatrix}\boldsymbol{x}\\ \boldsymbol{p}\end{bmatrix}, \tag{76}$$

where E is GPE, and EFM $\boldsymbol{E}$ and SM $\boldsymbol{U}$ respectively are

$$\boldsymbol{E}=\frac{1}{2}\begin{bmatrix}0 & \boldsymbol{I}-\boldsymbol{k}\\ \boldsymbol{I}-\boldsymbol{k} & 0\end{bmatrix},\qquad \boldsymbol{U}=\frac{1}{2}\begin{bmatrix}0 & \boldsymbol{I}+\boldsymbol{k}\\ -\boldsymbol{I}-\boldsymbol{k} & 0\end{bmatrix}. \tag{77}$$

The GKE and its flow are

$$K=\frac{1}{2}\begin{bmatrix}\dot{\boldsymbol{x}}^T & \dot{\boldsymbol{p}}^T\end{bmatrix}\begin{bmatrix}\dot{\boldsymbol{x}}\\ \dot{\boldsymbol{p}}\end{bmatrix}=\frac{1}{2}\begin{bmatrix}\dot{\boldsymbol{x}}^T & \dot{\boldsymbol{p}}^T\end{bmatrix}\begin{bmatrix}0 & \boldsymbol{I}\\ \boldsymbol{k} & 0\end{bmatrix}\begin{bmatrix}\boldsymbol{x}\\ \boldsymbol{p}\end{bmatrix}+\frac{1}{2}\dot{\boldsymbol{p}}^T\begin{bmatrix}0\\ \cos\widetilde{\omega}\tau\end{bmatrix},\qquad \dot{K}=\begin{bmatrix}\dot{\boldsymbol{x}}^T & \dot{\boldsymbol{p}}^T\end{bmatrix}\begin{bmatrix}\ddot{\boldsymbol{x}}\\ \ddot{\boldsymbol{p}}\end{bmatrix}. \tag{78}$$

The TAEFs for the chaotic system are given in Equations (32) and (33).

4.2.3. EFCF

The EFCFs are the eigenvalues of EFM $\boldsymbol{E}$, which are obtained by solving the equation

$$\begin{vmatrix}-\lambda\boldsymbol{I} & (\boldsymbol{I}-\boldsymbol{k})/2\\ (\boldsymbol{I}-\boldsymbol{k})/2 & -\lambda\boldsymbol{I}\end{vmatrix}=\lambda^2\left|-\lambda\boldsymbol{I}+\frac{1}{4}\lambda^{-1}(\boldsymbol{I}-\boldsymbol{k})^2\right|=\left|-\lambda^2\boldsymbol{I}+\frac{1}{4}(\boldsymbol{I}-\boldsymbol{k})^2\right|=0, \tag{79}$$

which, when the determinate formulation [62] is used, gives

$$\lambda_{1,2}=\pm\frac{1}{2}\sqrt{\frac{3+\sqrt{5}}{2}},\qquad \lambda_{3,4}=\pm\frac{1}{2}\sqrt{\frac{3-\sqrt{5}}{2}}. \tag{80}$$

Based on the orthogonality [30] of modes, we obtain

$$E=\begin{bmatrix}\boldsymbol{x}^T & \boldsymbol{p}^T\end{bmatrix}(\boldsymbol{E})\begin{bmatrix}\boldsymbol{x}\\ \boldsymbol{p}\end{bmatrix}=\sum_{I=1}^{4}\lambda_I\zeta_I^2, \tag{81}$$

where ζ_I denotes the coordinate along the principal direction I in PEFS spanned by the 4 eigenvectors. The GPE E is a Lyapunov function, and EFCFs play the roles of Lyapunov exponents to tackle the stability of the system about a point on the orbit. Equation (80) shows that this system has two positive and two negative Lyapunov exponents, so that it could have chaotic motions, which will be numerically investigated as follows.

4.3. Numerical Investigations

Using the MATLAB_R2024b with the opened programme [30], we investigate its orbits for the three cases of initial conditions: (a) $x_1=1=\dot{x}_1$, $x_2=0=\dot{x}_2$; (b) $x_1=0=\dot{x}_1$, $x_2=1=\dot{x}_2$; (c) $x_1=1=\dot{x}_1$, $x_2=1=\dot{x}_2$. Figure 12 shows the obtained results, where the orbits are, respectively, drawn for $(x_1,\dot{x}_1)$ and $(x_2,\dot{x}_2)$, due to the lack of a way to draw an orbit in 4-dimensional space. From these results, we can see that for three cases: (1) the orbits are non-closed curves with no repeating points; (2) the

time histories are mixed curves of two vibration components; (3) TAPE and TAKE, respectively, tend to their positive constants with average time increasing; (4) TAEFs, respectively, tend to zero with average time increasing. This is because the system has no LCM, so its period is infinite. Based on EFT, the motions are chaotic.

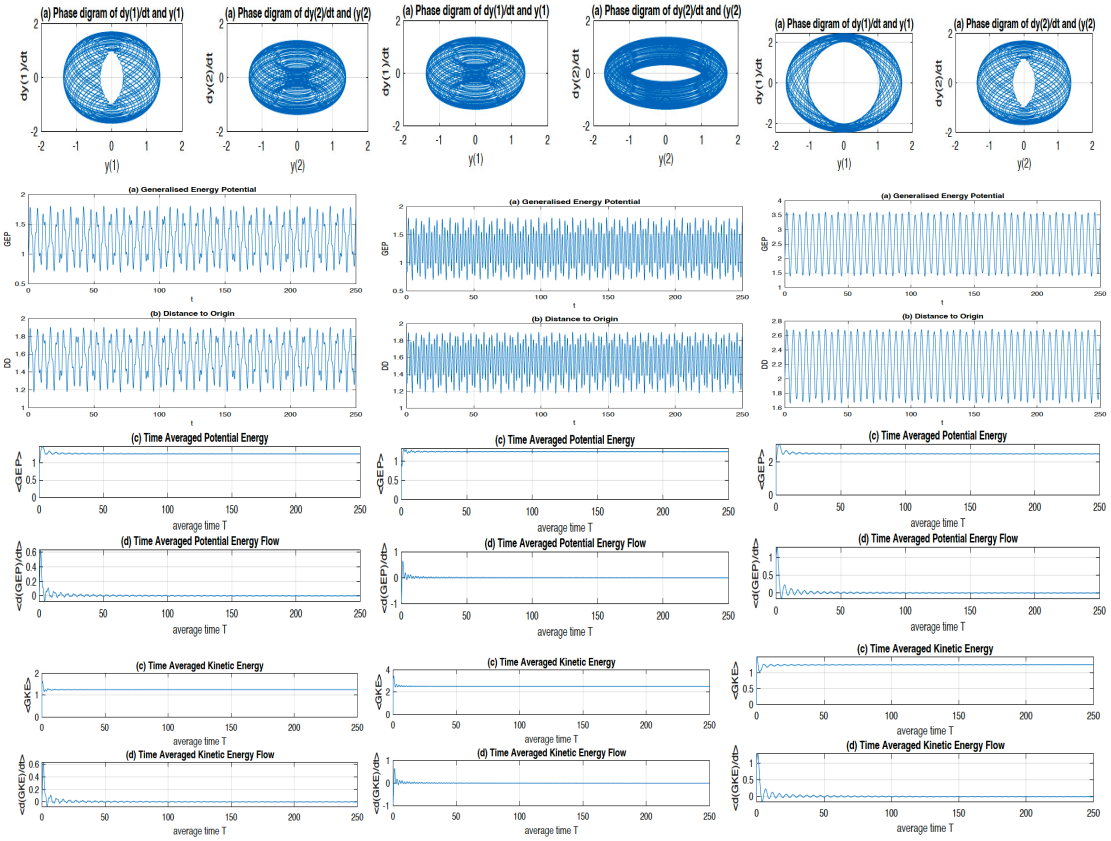


Figure 12. The orbits in phase space, the time histories of GPEs and distances to the origin, TAEFs with their TAPE/TAKE in free vibrations caused by initial conditions: left $x_1 = 1 = \dot{x}_1,\ x_2 = 0 = \dot{x}_2$; middle $x_1 = 0 = \dot{x}_1,\ x_2 = 1 = \dot{x}_2$; right $x_1 = 1 = \dot{x}_1,\ x_2 = 1 = \dot{x}_2$, where $y(1) = x_1,\ y(2) = x_2$.

4.4. Extension on Chaotic Motions in N-DOF Linear Systems

Based on the results mentioned in linear and QPS, as well as the principle of superposition of the solutions for linear systems, we may extend our findings into a general N-DOF linear system to conclude that chaotic motions in N-DOF linear systems appear if one of the following conditions is satisfied.

- If an N-DOF system has its N natural frequencies with no LCM, its non-damping free vibration caused by the initial conditions generally is chaotic, except the initial condition just excites part of the natural modes having their LCM. For example, the initial condition just forms one natural mode, so that the motion just has one natural frequency due to the orthogonality of natural modes.
- If an N-DOF damping system is excited by several external harmonic forces which have no LCM of their frequencies, after the free vibration components are damped, the stable forced vibration consists of the corresponding components with force frequencies supported by the principle of superposition; the motion is chaotic.

5. Discussion on Chaotic Motion in 1-DOF Linear System

In Section 3, we revealed the chaotic motions in the 1-DOF linear system based on EFT [30–32]. As indicated in [23] and a more detailed discussion in the book of EFT [30], there is no universally accepted mathematical definition of chaos. A commonly used

definition says that, for an NDS to be classified as chaotic, it must have some properties mentioned in Section 1, such as sensitive to initial conditions, topological transitivity and dense 'periodic' orbits. Currently, the widely accepted methods to identify chaotic motions are the Poincare maps and the Lyapunov exponents. To confirm the chaotic motion in the linear system identified by EFT in this paper, we further discuss this topic as follows.

- As far as we have learnt, the reported chaotic motions are in NDS, but not linear systems, which does not imply that there never exists chaos in linear systems, since no publications have demonstrated it.
- It has theoretically proved, see Equation (43), that the linear system tackled herein has one positive and another negative EFCF, which play the role of Lyapunov exponents with GPE as Lyapunov function, so that the Lyapunov exponents condition for chaos is satisfied.
- The vibration of the chaotic no-damping forced linear system consists of two components, as shown in Equations (45) and (46), one is free vibrations dependent on the initial conditions (x_0, p_0) and another is forced vibration dependent on force amplitude $\widetilde{F}$. Therefore, any minor change, such as initial conditions, will affect the orbits, so that the commonly accepted condition, sensitive to initial conditions, is no doubt satisfied. Furthermore, for a continuous initial condition set (x_0, p_0) (ρ) as a function of a real parameter ρ, letting ρ continuously changing in a defined domain, the corresponding dense orbits in phase space will be generated and transit from one orbit to a neighbouring one. Also, if we change the force amplitude, the orbits also have the following changes. The phase space volume strain Vs = 0, implying the obit volume is kept in a finite domain in phase space. These results confirm that the revealed chaotic motion in the linear system satisfies the current understanding of chaos.
- Poincare map: A radial line in the phase space orbits in Figure 4(II,III) and or Figure 5(II,III), where chaotic orbits are shown, can be considered as its Poincare section, and the intersecting points of this line with the orbits curves construct its Poincare map that is a set of points on this line, but no two ones at same place, since there is no CLM, so no common period for free vibration and force one.
- It is necessary to mention that, although the revealed chaotic motion can be generated by using the theoretical solution in Equations (45) and (46), we cannot obtain the exact value of each point, since it involves the evaluation of irrationals, of which the exact rational value is not known. Therefore, we cannot say that the orbit point of chaotic motion in a linear system can be exactly predicted.
- The tackled linear system showing chaotic motion is an ***idealised no-damping system, which normally does not exist in practical systems, since generally, damping cannot be avoided, which may be why chaotic motions have not been*** reported before this paper.

6. Conclusions and Further Research Topics

We have completed a detailed investigation on chaotic/periodic motions in linear and NDSs based on EFT, by which a chaotic motion is considered as a periodical motion with infinite period. The LCM of periods for frequencies of vibration components may be a key factor in identifying chaotic motions in the related cases tackled in the paper. The research has revealed the chaotic motions in 1-DOF dynamic systems. (a) For a linear, non-damped forced system, a type of chaotic motion has been discovered when there is no LCM for the periods of natural and force frequencies, implying that there exist chaotic motions in linear systems, addressing the question proposed in the introduction of the paper. (b) For a 1-DOF nonlinear non-damping forced system with the nonlinear stiffness in the form of γx^2, $(\gamma > 0)$, both the free motion by initial conditions and the composed motions with the forced one caused by the given excitation are chaotic; while, when the damping is added,

the free vibration is gradually damped to zero, but the forced vibration consists of different frequency components showing chaotic characteristics. (c) For a 1-DOF system of natural frequency 1 with nonlinear amping $2\varepsilon(\dot{x}) = -2 + \dot{x} + \dot{x}^2$, $\varepsilon(\dot{x}) < 0$, $\varepsilon(\dot{x})^2 < 1$, the motion of free vibration caused by the initial conditions ($x_0 = 1$, $p_0 = 0$) along a non-repeating orbit towards a zero energy-flow limit circle of $\dot{E} = 0$, $p = -1$. The chaotic orbits discovered above have been shown by the curves in the phase space. It has been shown that GPE and EFCFs, respectively, play the roles of Lyapunov functions and exponents to tackle NDSs in EFT, so that by adopting energy flow variables to investigate NDS, we no longer need to seek a Lyapunov function. The revealed Chaotic motion in a linear system is further discussed based on the Poincare map, Lyapunov exponents, as well as commonly accepted knowledge to confirm the finding is acceptable.

It has been realised that the studied linear 1-DOF systems of no LCMs belong to a type of QPS, from EFT, the motion of a QPS is chaotic, which is examined by numerically investigating a 2-DOF example. The idea to reveal possible chaotic motions for QRS and 1DOF linear systems might be extended to general N-DOF linear systems.

The results developed in the paper may suggest that LCMs could be an important factor in identifying chaotic motions to address the second question proposed in the introduction. A system with no LCM can be considered its LCM being infinite, which is why the chaotic motion is imaged as a periodical one with infinite period. Although this type of chaotic oscillation is a summation of given harmonic functions, we cannot say that the chaotic motion can be predicated, since it involves irrational numbers, which cannot give the exact rational position of each orbit point.

The following research directions may be proposed for readers to further develop EFT to deal with more complex practical dynamical systems.

- LCM applicable cases are given by the mentioned linear and linear examples to identify possible chaotic motions. We have assumed the possible chaotic motion cases for general N-DOF linear systems in Section 4.3. However, we have not tackled more general NDS using LCM, which may be investigated by readers.
- We discuss the chaotic motions in a linear system according to the understanding of chaos knowledge by the author, but we cannot fully check all the different chaos reports to compare them, due to the author's limited knowledge. The interesting readers might possibly tackle it using other chaotic information reported but not mentioned in this paper.
- For a QPS, its phase space orbit and time history are unique, which does not involve EFT. We only find its chaotic orbit behaviour due to no CLM, i.e., no common period of its components. Therefore, a time history point and its corresponding phase space orbit point never coincide with others, showing chaotic behaviour according to EFT. Only a 2DOF non-damping example is examined in this paper, and its extension has not given examples, so that more possible cases may be performed by readers.
- To the author's current knowledge of EFT, the provided mathematical demonstration on chaos was given in [30–37] and summarised in Section 2.5.4. Possible other demonstrations may be developed by readers, for example, to reveal the connection between EFT-based criteria and widely accepted topological entropy/Lyapunov function. The author, being not an expert in pure mathematics, while initially reading the related publications [63,64], might give the following personal understandings on this topic: (a) GPE E automatically is a Lyapunov function, and EFCFs λ_I are Lyapunov exponents to tackle stabilities, periodical/chaotic motions of NDSs; (b) GPE E and GKE K are two metrics, respectively, for orbit field and its tangent space; (c) flows of GPE ($\dot{E}$) and GKE ($\dot{K}$) define their variations, i.e., the evolution of distinguishable orbits over time; (d) the four-time integrations in Equations (32) and (33) could play the

roles of two topological entropies. The author deeply wishes experts in mathematics to confirm or correct my initial understanding above, and possibly to give an exact mathematical demonstration. I am looking forward to reading these further new contributions of EFT.

Author Contributions: Conceptualization, J.T.X.; Methodology, J.T.X. and W.D.; Validation, W.D.; Formal analysis, J.T.X.; Investigation, J.T.X.; Writing—original draft, J.T.X.; Writing—review & editing, W.D.; Project administration, W.D. All authors have read and agreed to the published version of the manuscript.

Funding: This research received no external funding.

Data Availability Statement: The original contributions presented in this study are included in the article. Further inquiries can be directed to the corresponding author.

Acknowledgments: The authors acknowledges the journal editors and three referees for their hard work to read and check the manuscript, and for giving very useful advice to modify the paper to be accepted for publication.

Conflicts of Interest: The authors declare no conflicts of interest.

References

1. Poincaré, J.H. Sur le problème des trois corps et les équations de la dynamique. *Acta Math.* **1890**, *13*, A3–A270. [CrossRef]
2. Diacu, F.; Holmes, P. *Celestial Encounters: The Origins of Chaos and Stability*; Princeton University Press: Princeton, NJ, USA, 1996.
3. Lorenz, E.N. Deterministic non-periodic flow. *J. Atmos. Sci.* **1963**, *20*, 130–141. [CrossRef]
4. Hirsch, M.W.; Smale, S. *Differential Equations, Dynamical Systems, and Linear Algebra*; Academic Press: New York, NY, USA, 1974.
5. Sparrow, C. *The Lorenz Equations: Bifurcations, Chaos, and Strange Attractors*; Springer: New York, NY, USA, 1982.
6. Guckenheimer, J.; Holmes, P. *Nonlinear Oscillations, Dynamical Systems, and Bifurcations of Vector Fields*; Springer: New York, NY, USA, 1983.
7. Thompson, J.M.T.; Stewart, H.B. *Nonlinear Dynamics and Chaos, Geometrical Methods for Engineers and Scientists*; John Wiley: Chichester, UK, 1986.
8. Abraham, N.B.; Arecchi, F.T.; Lugiato, L.A. (Eds.) *Instabilities and Chaos in Quantum Optics II: Proceedings of the NATO Advanced Study Institute, II Ciocco, Italy, June 28–July 7, 1987*; Springer: New York, NY, USA, 1988.
9. Kellert, S.H. *In the Wake of Chaos: Unpredictable Order in Dynamical Systems*; University of Chicago Press: Chicago, IL, USA, 1993.
10. Strogatz, S.H. *Nonlinear Dynamics and Chaos*; Perseus Publishing: Cambridge, MA, USA, 1994.
11. Alligood, K.T.; Sauer, T.; Yorke, J.A. *Chaos: An Introduction to Dynamical Systems*; Springer: New York, NY, USA, 1997.
12. Serletis, A.; Gogas, P. The north American gas markets are chaotic. *Energy J.* **1999**, *20*, 83–103. [CrossRef]
13. Gribbin, J. *Deep Simplicity: Bringing Order to Chaos and Complexity*, 1st ed.; Random House: New York, NY, USA, 2004.
14. Kyrtsou, C.; Labys, W. Evidence for chaotic dependence between US inflation and commodity prices. *J. Macroecon.* **2006**, *28*, 256–266. [CrossRef]
15. Ivancevic, V.G.; Ivancevic, T.T. *Complex Nonlinearity: Chaos, Phase Transitions, Topology Change, and Path Integrals*; Springer: New York, NY, USA, 2008.
16. Werndl, C. What are the new implications of chaos for unpredictability? *Br. J. Philos. Sci.* **2009**, *60*, 195–220. [CrossRef]
17. Stroyatz, S.H. *Nonlinear Dynamics and Chaos with Applications to Physics, Biology, Chemistry, and Engineering*; Westview Press: Boulder, CO, USA, 2001.
18. Layek, G.C. *An Introduction to Dynamical Systems and Chaos*; Springer Nature: Berlin/Heidelberg, Germany, 2024.
19. Yoshida, Z. *Nonlinear Science*; Springer: Berlin/Heidelberg, Germany, 2010.
20. Machado, J.A.; Luo, A.C.J.; Barbosa, R.S.; Manuel, M.F.; Figueiredo, L.B. *Nonlinear Science and Complexity*; Springer: Dordrecht, The Netherlands, 2011.
21. Afraimovich, V.; Luo, A.C.J.; Fu, X. *Nonlinear Dynamics and Complexity*; Springer: Berlin/Heidelberg, Germany, 2014.
22. Pinto, C.M.A. *Nonlinear Dynamics and Complexity*; Springer Nature: Berlin/Heidelberg, Germany, 2022.
23. Hasselblatt, B.; Katok, A. *A First Course in Dynamics: With a Panorama of Recent Developments*; Cambridge University Press: Cambridge, UK, 2003.
24. Zhang, J.; Chen, L.-Q. Complex dynamics of a harmonically excited structure coupled with a nonlinear energy sink. *Acta Mech. Sin.* **2017**, *33*, 801–822. [CrossRef]

25. Guo, H.; Yang, T.; Chen, Y.; Chen, L.-Q. Singularity analysis on vibration reduction of a nonlinear energy sink system. *Mech. Syst. Signal Process.* **2022**, *173*, 109074. [CrossRef]
26. Ding, H.; Chen, L.-Q. Designs, analysis, and applications of nonlinear energy sinks. *Nonlinear Dyn.* **2020**, *100*, 3061–3107. [CrossRef]
27. Saeed, A.S.; Nasar, R.A.; AL-Shudeifat, M.A. A review on nonlinear energy sinks: Designs, analysis and applications of impact and rotary types. *Nonlinear Dyn.* **2023**, *111*, 1–37. [CrossRef]
28. Shao, Y.F.; Ji, J.C.; Ding, H. Dynamics and vibration reduction performance of a cross-type motion amplified nonlinear energy sink. *Acta Mech. Sin.* **2025**, *41*, 524948. [CrossRef]
29. Zhang, Y.; Wen, H.; Hu, H.; Jin, D. A novel quasi-zero stiffness isolator with designable stiffness using cam-roller-spring-rod mechanism. *Acta Mech. Sin.* **2025**, *41*, 524210.
30. Xing, J.T. *Energy Flow Theory of Nonlinear Dynamical Systems with Applications*; Springer: Berlin/Heidelberg, Germany, 2015.
31. Xing, J.T. Energy flow characteristics of periodical orbits on nonlinear dynamical systems. In Proceedings of the 10th European Nonlinear Dynamics Conference, Enoc2020+2, Lyon, France, 17–22 July 2022. Available online: https://enoc2020.scienceconf.org:enoc2020:376976 (accessed on 17 July 2022).
32. Xing, J.T. Generalised energy conservation law for chaotic phenomena. *Acta Mech. Sin.* **2019**, *35*, 1257–1268. [CrossRef]
33. Qin, L.; Qin, H.; Xing, J.T. Energy flow characteristics of friction-induced nonlinear vibrations in a water-lubricated bearing-shat coupled system. *Acta Mech. Sin.* **2021**, *37*, 679–704. [CrossRef]
34. Xing, J.T.; Sun, Z.; Zhou, S.; Tan, M. Dynamic interactions of an integrated vehicle-electromagnetic energy harvester-tire system subject to uneven road excitations. *Acta Mech. Sin.* **2017**, *33*, 440–456. [CrossRef]
35. Xing, J.T.; Qin, L. A railway vehicle-electromagnetic suspension coupling system for vibration reduction with energy harvesting, Paper ID 23. In Proceedings of the 29th International Congress on Sound and Vibration, Prague, Czech Republic, 9–13 July 2023.
36. Zhang, C.; Liu, Y.; Zhu, X.; Li, T.; Xing, J.T. Vibration reduction and energy harvesting of a human-seat-boat-water dynamic interaction system excited by waves. *Ocean Eng.* **2023**, *288*, OE_116010. [CrossRef]
37. Xing, J.T. Developments of Energy Flow Theory for Nonlinear Dynamical Systems and Applications to Relativistic Dynamics. In *Book Abstracts, the IUTAM Symposium on Nonlinear Dynamics for Design of Mechanical Systems Across Different Length/Time Scales, Tsukuba Science City, Japan, 31 July–4 August 2023*; Springer: Cham, Switzerland, 2023. Available online: https://sites.google.com/view/nonlinear-dynamics (accessed on 31 July 2023).
38. Van der Pol, B. A theory of the amplitude of free and forced triode vibrations. *Radio Rev.* **1920**, *1*, 701–710; 754–762.
39. Parlitz, U.; Lauterborn, W. Period-doubling cascades and Devil's staircases of Van Der Pol oscillator. *Phys. Rev.* **1987**, *A36*, 1428–1434. [CrossRef]
40. Moon, F.C.; Holmes, P.J. A magnetoelastic strange attractor. *J. Sound Vib.* **1979**, *65*, 285–296. [CrossRef]
41. Cao, Q.; Wiercigroch, M.; Pavlovskaia, E.E.; Grebogi, C.; Thompson, J.M.T. SD oscillator, SD attractor and its applications. *J. Vib. Eng.* **2007**, *20*, 454–458.
42. Cao, Q.; Wiercigroch, M.; Pavlovskaia, E.E.; Grebogi, C.; Thompson, J.M.T. Piecewise linear approach to an archetypal oscillator for smooth and discontinuous dynamics. *Philos. Trans. R. Soc. Lond. A* **2008**, *366*, 635–652.
43. Williams, R.F. *The Structure of Lorenz Attractors*; Lecture Notes in Math; Springer: Berlin/Heidelberg, Germany, 1977; Volume 615.
44. Lanford, O.E. *Computer Pictures of Lorenz Attractor*; Springer: Berlin/Heidelberg, Germany, 1977.
45. Rössler, O.E. An equation for continuous chaos. *Phys. Lett. A* **1976**, *57*, 397–398. [CrossRef]
46. Xing, J.T. Solutions of three-body problem based on an equivalent system approach. *Acta Mech. Sin.* **2026**, *42*, 524942. [CrossRef]
47. Xing, J.T. Chaotic motions in Newton's gravity field revealed from energy flow investigations. *Acta Mech. Sin.* **2026**, *42*, 525511. [CrossRef]
48. Malik, S.A.; Mir, A.H. Discrete multiplierless implementation of fractional order hindmarsh–rose model. *IEEE Trans. Emerg. Top. Comput. Intell.* **2021**, *5*, 792–802. [CrossRef]
49. Onuki, K.; Cho, K.; Horio, Y.; Miyano, T. Secret-key exchange through synchronization of randomized chaotic oscillators aided by logistic hash function. *IEEE Trans. Circuits Syst. I Regul. Pap.* **2022**, *69*, 1655–1667. [CrossRef]
50. Chen, Y.; Shi, Z.; Lin, C. Some criteria for the global finite-time synchronization of two Lorenz-Stenflo systems coupled by a new controller. *Appl. Math. Model.* **2014**, *38*, 4076–4085. [CrossRef]
51. Liu, X.; Zhao, L.; Jin, J. A noise-tolerant fuzzy-type zeroing neural network for robust synchronization of chaotic systems. *Concurr. Comput. Pract. Exp.* **2024**, *36*, e8218. [CrossRef]
52. Jin, J.; Chen, W.; Ouyang, A.; Fei Yu, F.; Liu, H. A Time-Varying Fuzzy Parameter Zeroing Neural Network for the Synchronization of Chaotic Systems. *IEEE Trans. Emerg. Top. Comput. Intell.* **2024**, *8*, 364–376. [CrossRef]
53. Majhi, S.; Perc, M.; Ghosh, D. Dynamics on higher-order networks: A review. *J. R. Soc. Interface* **2022**, *19*, 20220043. [CrossRef] [PubMed]

54. Yang, Q.; Teng, W.; Guo, K.; Wang, T.; Zhao, L.; Hui, Y.; Liu, M. Large Eddy Simulation of self-excited forces in forced-vibration square prisms: Lock-In regime dynamics and vortex shedding modulation. *J. Wind Eng. Ind. Aerodyn.* **2026**, *270*, 106338. [CrossRef]
55. Cui, W.; Zhao, L.; Ge, Y.; Xu, K. A generalized van der Pol nonlinear model of vortex-induced vibrations of bridge decks with multistability. *Nonlinear Dyn.* **2024**, *112*, 259–272.
56. Xing, J.T.; Dai, W. Chaotic motions in 1-D linear/nonlinear and quasi-periodical dynamic systems revealed by energy-flow investigations. *Preprint* **2026**. [CrossRef]
57. Xing, J.T. *Fluid-Solid Interaction Dynamics, Theory, Variational Principles, Numerical Methods, and Applications*; Elsevier Academic Press: New York, NY, USA, 2019.
58. Wikipedia(a). Duffing Equation. 2026. Available online: https://en.wikipedia.org/wiki/Duffing_equation (accessed on 10 July 2026).
59. Wikipedia(b). Poincare-Bendixson Theorem. 2026. Available online: https://en.wickipedia.org/wiki/Poincaré–Bendixson_theorem (accessed on 10 July 2026).
60. Sprott, J.C. *Elegant Chaos: Algebraically Simple Chaotic Flows*; World Scientific: Singapore, 2010.
61. Samoilenko, A.M. Quasiperiodic oscillations. *Scholarpedia* **2007**, *2*, 1783. [CrossRef]
62. Zhang, F. *The Schur Complement and Its Applications*; Springer: Berlin/Heidelberg, Germany, 2005.
63. Wikipedia(c). Topological Entropy. 2026. Available online: https://en.wickipedia.org/wiki/Topological_entropy (accessed on 10 July 2026).
64. Butt, K. An Introduction to Topological Entropy. 2014. Available online: https://math.uchicago.edu (accessed on 10 July 2026).

Disclaimer/Publisher's Note: The statements, opinions and data contained in all publications are solely those of the individual author(s) and contributor(s) and not of MDPI and/or the editor(s). MDPI and/or the editor(s) disclaim responsibility for any injury to people or property resulting from any ideas, methods, instructions or products referred to in the content.